



CERN-PH-TH-2014-265

PREPARED FOR SUBMISSION TO JHEP

Reference results for time-like evolution up to $\mathcal{O}(\alpha_s^3)$

Valerio Bertone,^a Stefano Carrazza,^{a,b,1} Emanuele R. Nocera.^c

^a*PH Department, TH Unit,
CERN, CH-1211 Geneva 23, Switzerland*

^b*Dipartimento di Fisica, Università di Milano and INFN, Sezione di Milano,
Via Celoria 16, I-20133 Milano, Italy*

^c*Dipartimento di Fisica, Università di Genova and INFN, Sezione di Genova,
Via Dodecaneso 33, I-16146 Genova, Italy*

E-mail: valerio.bertone@cern.ch, stefano.carrazza@mi.infn.it,
emanuele.nocera@edu.unige.it

ABSTRACT: We present high-precision numerical results for time-like Dokshitzer-Gribov-Lipatov-Altarelli-Parisi evolution in the $\overline{\text{MS}}$ factorisation scheme, for the first time up to next-to-next-to-leading order accuracy in quantum chromodynamics. First, we scrutinise the analytical expressions of the splitting functions available in the literature, in both x and N space, and check their mutual consistency. Second, we implement time-like evolution in two publicly available, entirely independent and conceptually different numerical codes, in x and N space respectively: the already existing APFEL code, which has been updated with time-like evolution, and the new MELA code, which has been specifically developed to perform the study in this work. Third, by means of a model for fragmentation functions, we provide results for the evolution in different factorisation schemes, for different ratios between renormalisation and factorisation scales and at different final scales. Our results are collected in the format of benchmark tables, which could be used as a reference for global determinations of fragmentation functions in the future.

KEYWORDS: fragmentation functions, time-like evolution, high-precision computation

ARXIV EPRINT: [1501.00494](https://arxiv.org/abs/1501.00494)

¹Corresponding author.

Contents

1	Introduction	1
2	Time-like evolution	3
3	Numerical implementation and benchmark	6
3.1	The codes	7
3.2	The setup	7
3.3	The results	8
4	Conclusions and outlook	11
A	Numerical Results	12
B	The MELA evolution code	12

1 Introduction

In the framework of perturbative Quantum Chromodynamics (QCD), parton-to-hadron Fragmentation Functions (FFs) encode the information on how quarks and gluons are turned into hadrons [1, 2]. Their precise knowledge is an essential ingredient in the quantitative description of any hard-scattering process involving identified hadrons in the final state. Like Parton Distribution Functions (PDFs), FFs are non-perturbative quantities and, as such, they have to be determined from experimental data, typically in a global QCD analysis of a large variety of processes [3, 4]. These analyses are all based on factorisation [5], which allows one to compute the relevant hard-scattering matrix elements perturbatively, and to absorb the collinear singularities arising from the masslessness of partons into FFs. After factorisation, perturbative QCD corrections lead FFs to depend on the factorisation scale μ_F , and this dependence obeys time-like Dokshitzer-Gribov-Lipatov-Altarelli-Parisi (DGLAP) evolution equations [6–9].

Available experimental data to be included in a global QCD analysis of FFs span several orders of magnitude in energy. Beside rather old measurements (see ref. [4] for a review), new high-precision data are being produced copiously. On the one hand, they include multiplicities in fixed-target semi-inclusive deep-inelastic scattering (SIDIS) from HERMES [10] and COMPASS [11] experiments at $1.1 \leq Q^2 \leq 7.4 \text{ GeV}^2$ and $1.2 \leq Q^2 \leq 22.4 \text{ GeV}^2$ respectively. On the other hand, they include production cross-sections of light hadrons in e^+e^- collisions from BELLE [12] and BABAR [13] experiments at a center-of-mass energy $\sqrt{s} \simeq 10.5 \text{ GeV}$, and in pp collisions from STAR [14] and PHENIX [15] experiments at $\sqrt{s} = 200 \text{ GeV}$ and from CMS[16, 17] and ALICE [18] experiments up to

$\sqrt{s} = 7$ TeV. Large Hadron Collider (LHC) data extend to unprecedented large values the energy reach, which will be even pushed forward by the future LHC Run-II.

In order to determine FFs from these data sets, the evolution programs required for the multi-parameter global QCD analyses have to be numerically and conceptually under control. In principle, the demanded accuracy is the same as for PDFs: indeed, FFs and PDFs are on the same footing, and eventually they could be determined simultaneously in a fit to experimental data. This may be of particular interest in the case of spin-dependent PDFs, since a large amount of the experimental information used for their determination comes from SIDIS data with longitudinally polarised beams and targets. In this case, the potential cross-talk between spin-dependent PDFs and FFs could then be profitably addressed in a fit of both these quantities based on a mutually consistent methodology.

So far, high-precision numerical results for time-like evolution have not been presented in a systematic way. In very much the same spirit of previous studies for space-like evolution [19, 20], the goal of this paper is to fill this gap: specifically, we present results obtained in the $\overline{\text{MS}}$ factorisation scheme and, for the first time, up to next-to-next-to-leading order (NNLO) accuracy in QCD. Our study aims at providing a reference for future global QCD analyses of FFs.

Our goal is achieved in three steps. First, we check the mutual correspondence of time-like splitting functions in the literature in both x and N space whenever available. Second, we implement them in two entirely independent and conceptually different evolution programs: **APFEL** (A PDF Evolution Library) [21, 22], an already existing evolution package which in version 2.3.0 has been updated with time-like evolution, and **MELA** (Mellin Evolution LibrAry), a new program which has been developed specifically for the purpose of this paper. Third, we use a model for FFs with a sufficient degree of realistic behavior in order to obtain our reference results. Provided perfectly controlled conditions, obtaining the same results irrespective of the procedure followed in the two codes provides a strong check of the correctness of both our implementations and our results.

Note that time-like evolution is performed in the $\overline{\text{MS}}$ factorisation scheme by two publicly available programs, **QCDnum** [23] and **ffevol** [24], and by private codes used for recent global determinations of FFs [25–27], though only up to next-to-leading order (NLO) accuracy. Furthermore, these codes differ among each other for physical and technical assumptions, hence a comparison between the results obtained either with **QCDnum** and **ffevol** or with one of these programs and published parameterisations is not straightforward (or even not possible). In this respect, our results provide a reference for future comparisons with these codes, calling for a dedicated effort beyond the scope of this work.

The paper is organised as follows. In section 2, we review the structure of the DGLAP evolution equations, and we scrutinise the expressions of the time-like splitting functions available in the literature. In section 3, we describe the numerical implementation of the time-like evolution in **MELA**, we discuss the setup conditions for our benchmark versus **APFEL**, and we present corresponding results and accuracy. Two appendices complete our paper. In appendix A, we collect the numerical results of our study in the format of benchmark tables. Finally, in appendix B, we provide a minimal set of instructions for downloading and running the **MELA** benchmark code.

2 Time-like evolution

The evolution of parton-to-hadron FFs is described by $2n_f + 1$ DGLAP equations

$$\frac{\partial}{\partial \ln \mu_F^2} D_i^h(x, \mu_F^2) = \sum_j \int_x^1 \frac{dy}{y} P_{ji}(y, \alpha_s(\mu_F^2)) D_j^h\left(\frac{x}{y}, \mu_F^2\right), \quad (2.1)$$

where n_f is the number of active flavours, the index j runs over partons, D_i^h is the FF for the parton i to fragment into a hadron h , x is the scaled energy of the hadron h (i.e. the fraction of the parton four-momentum taken by the hadron h), μ_F is the factorisation scale, α_s is the QCD running coupling, and P_{ji} are the time-like splitting functions. These allow for a perturbative expansion of the form:

$$P_{ji}(y, \alpha_s) = \sum_{k=0} a_s^{k+1} P_{ji}^{(k)}(y), \quad (2.2)$$

where we have defined $a_s = \alpha_s/(4\pi)$. From considerations based on charge conjugation and flavour symmetry, eqs. (2.1) are usually rewritten into $2n_f - 1$ equations

$$\frac{\partial}{\partial \ln \mu_F^2} D_{\text{NS};\pm,v}^h(x, \mu_F^2) = P^{\pm,v}(x, \mu_F^2) \otimes D_{\text{NS};\pm,v}^h(x, \mu_F^2) \quad (2.3)$$

describing the independent evolution of non-singlet quark FF combinations, $D_{\text{NS};\pm}^h = (D_{q_i}^h \pm D_{\bar{q}_i}^h) - (D_{q_j}^h \pm D_{\bar{q}_j}^h)$ and $D_{\text{NS};v}^h = \sum_{i=1}^{n_f} (D_{q_i}^h - D_{\bar{q}_i}^h)$, and a system of two coupled equations

$$\frac{\partial}{\partial \ln \mu_F^2} \begin{pmatrix} D_{\Sigma}^h(x, \mu_F^2) \\ D_g^h(x, \mu_F^2) \end{pmatrix} = \begin{pmatrix} P^{\text{qq}} & 2n_f P^{\text{gq}} \\ \frac{1}{2n_f} P^{\text{qg}} & P^{\text{gg}} \end{pmatrix} \otimes \begin{pmatrix} D_{\Sigma}^h(x, \mu_F^2) \\ D_g^h(x, \mu_F^2) \end{pmatrix} \quad (2.4)$$

describing the evolution of gluon and singlet fragmentation functions, D_g^h and $D_{\Sigma}^h = \sum_{i=1}^{n_f} (D_{q_i}^h + D_{\bar{q}_i}^h)$. The shorthand notation \otimes stands for the convolution product

$$f(x) \otimes g(x) \equiv \int_x^1 \frac{dy}{y} f(y) g\left(\frac{x}{y}\right). \quad (2.5)$$

The solution of eqs. (2.1) can be performed either in x or in N space; in N space, the system of integro-differential equations (2.1) becomes a system of Ordinary Differential Equations (ODEs) of the form

$$\frac{\partial}{\partial \ln \mu_F^2} D_i^h(N, \mu_F^2) = \sum_j P_{ji}(N, \alpha_s(\mu_F^2)) D_j^h(N, \mu_F^2). \quad (2.6)$$

The splitting functions in the two spaces can be related to each other via the Mellin transform

$$P_{ji}(N, \alpha_s) = \int_0^1 dy y^{N-1} P_{ji}(y, \alpha_s), \quad N \in \mathbb{C}, \quad (2.7)$$

and its inverse

$$P_{ji}(y, \alpha_s) = \frac{1}{2\pi i} \int_{c-i\infty}^{c+i\infty} dN y^{-N} P_{ji}(N, \alpha_s), \quad (2.8)$$

where the real number c has to lie to the right of the rightmost singularity of P_{ji} in the complex plane. Fragmentation functions in x and N space are related with each other by the same transformations as in eqs. (2.7)-(2.8).

At leading order (LO), time-like splitting functions are identical to their space-like counterparts, while they differ at higher orders. At NLO, explicit expressions for the complete set of time-like splitting functions in eqs. (2.3)-(2.4) are collected in refs. [28, 29] (x space), in ref. [30] (N space) and ref. [31] (both x and N space), though with rather different notations.¹ All results are given in the $\overline{\text{MS}}$ factorisation scheme.

Time-like splitting functions have been computed up to $\mathcal{O}(\alpha_s^3)$, *i.e.* NNLO accuracy, always in the $\overline{\text{MS}}$ factorisation scheme in refs. [35–37]. An uncertainty still remains on the exact form of $P_{\text{qg}}^{(2)}$. Indeed, this was determined by means of a relation between known NLO evolution kernels for photon- and Higgs-exchange structure functions in deep-inelastic scattering, and their counterparts in semi-inclusive annihilation [32, 38], supplemented with constraints arising from momentum sum rule and supersymmetric relations for the choice $C_A = C_F = n_f$ of colour factors. The latter fix the form of $P_{\text{qg}}^{(2)}$ except for the offset quantified by Eq. (38) in ref. [37], which does not affect the logarithmic behaviour of $P_{\text{qg}}^{(2)}$ at small and large momentum fractions [37] and consequently the validity of our study. Note finally that coefficient functions are known at NNLO only for e^+e^- annihilation [31, 39–41]: this will thus limit the potential of a global determination of fragmentation functions at NNLO.

For doubt’s sake, we checked that all the aforementioned results, in both x and N space, fully agree with each other up to NNLO accuracy. At LO, such a check is straightforward due to the extreme simplicity of the expressions involved, and we found perfect agreement among all the results considered. At NLO and NNLO, instead, time-like splitting functions are much more complicated than at LO. Also, at NLO the check is complicated by the fact that different notations, not directly comparable, and different FF basis are used in refs. [29–31]. Be that as it may, we considered the basis of refs. [31, 35–37]: at NLO, this is $\{P^+, P^-, P^{\text{ps}}, P^{\text{qg}}, P^{\text{gq}}, P^{\text{gg}}\}$, at NNLO, this is $\{P^+, P^-, P^{\text{v}}, P^{\text{ps}}, P^{\text{qg}}, P^{\text{gq}}, P^{\text{gg}}\}$.² This corresponds to the basis entering eqs. (2.3)-(2.4), provided that $P^{\text{qg}} = P^+ + P^{\text{ps}}$. We refer to chapter 4 of ref. [29] for another example of FF basis.

At NLO, we carried out the comparison in two steps. First, we checked that the x -space results in refs. [29, 31] and the N -space results in refs. [30, 31] are identical. We performed this check both analytically and numerically. On the one hand, in order to deal with the analytic notation in ref. [31], we have used the definitions of harmonic polylogarithms and harmonic sums provided in refs. [42, 43]. On the other hand, we have used the package presented in ref. [44] to handle harmonic sums numerically. Second, we checked that the x -space results in ref. [29] correspond to the N -space results in ref. [30], and that x - and N -space results in ref. [31] correspond to each other. We performed this check numerically,

¹Results in ref. [29] were obtained for the first time in ref. [28]. Well-known misprints in ref. [28] have been amended in ref. [29], see also refs. [32, 33]. Note that N -space results in ref. [30] were obtained by applying the Mellin transform, eq. (2.7), to the x -space results in ref. [28], while those in ref. [31] were derived directly in N space using the method presented in ref. [34].

²Note that, at NLO, there are only six independent splitting functions because $P^{\text{v}} = P^-$.

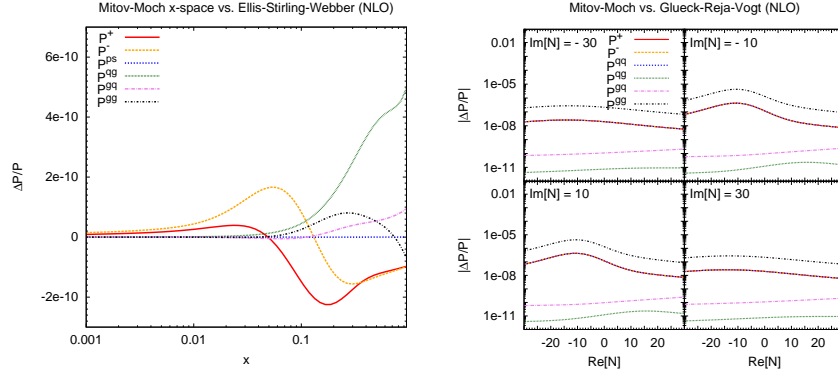


Figure 1: (Left panel). The relative difference $\Delta P/P$ between the x -space splitting functions of ref. [31] and those of ref. [29]. (Right panel). The absolute relative difference $|\Delta P/P|$ between the N -space splitting functions of ref. [31] and those of ref. [30].

by transforming the N -space expressions in x space, and by comparing the results with the corresponding x -space expressions (for details about the implementation of the inverse Mellin transform, see section 3.1 below).

At NNLO, we checked that the x - and N -space expressions provided in refs. [35–37], and available in ref. [45] in the format of **Fortran** subroutines, correspond to each other. Again, we performed this check numerically, by transforming the N -space expressions in x space, and by comparing the results with the corresponding x -space expressions. Note that we considered the approximate representation (or parameterisation) of NNLO time-like splitting functions provided in ref. [45], consistently in x and N space. Indeed, the exact expressions of the NNLO splitting functions are rather complex and these will lead to very lengthy computations once implemented in a code for numerical evolution like **APFEL**. It was checked in ref. [37] that, except for values of x very close to zeros of the splitting functions, such approximate expressions deviate from the exact ones by less than one part in a thousand.

In the left panel of figure 1, we show the relative difference between the x -space splitting functions of ref. [29] and those of ref. [31] over a sensible range in x . In the right panel of figure 1, we show the absolute value of the relative difference between the N -space splitting functions of ref. [30] and those of ref. [31] over a wide portion of the complex plane. In the left panel of figure 2, we show the relative difference between the exact x -space splitting functions in ref. [29] and the numerical inversion of the N -space expressions of ref. [30] (at NLO). In the central panel of figure 2, we show the same comparison but for the splitting functions in ref. [31] (at NLO). In the right panel of figure 2, we show the same comparison, but for the NNLO splitting functions in refs. [35–37, 45].

The results displayed in figures 1 and 2 allow us to draw the following conclusions.

- The agreement between the expressions of time-like splitting functions at NLO, in x and N space separately, is optimal. In the x -space case (left plot in figure 1), the relative difference between them is $\Delta P/P \sim 10^{-10}$. In the N -space case (right plot in figure 1), the range for the absolute relative difference between them is $10^{-11} \lesssim$

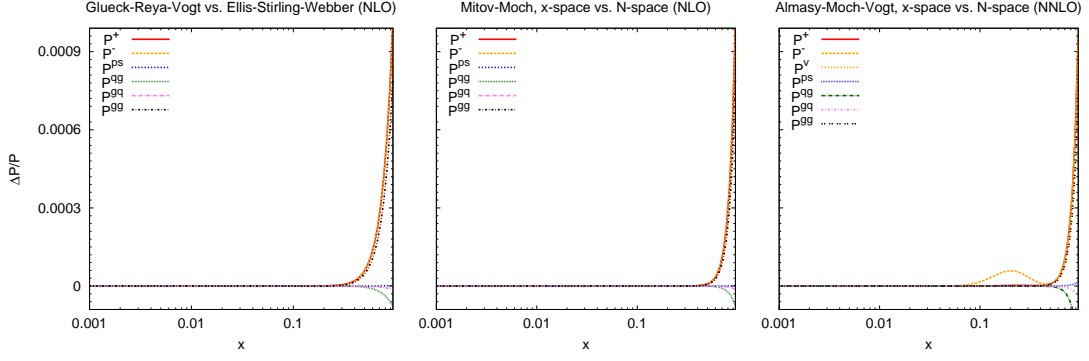


Figure 2: (Left panel). The relative difference $\Delta P/P$ between the x -space splitting functions of ref. [29] and the inverse Mellin transform of the N -space splitting functions from ref. [30]. (Central panel). The relative difference $\Delta P/P$ between the x -space and N -space splitting functions of ref. [31] (at NLO). (Right panel) The relative difference $\Delta P/P$ between the x -space and N -space splitting functions of refs. [35–37, 45] (at NNLO).

$|\Delta P/P| \lesssim 10^{-5}$. The fact that the values of $|\Delta P/P|$ in the N -space case cover a larger spread than the values of $\Delta P/P$ in the x -space case is a consequence of the numerical evaluation of harmonic sums with the package provided in ref. [44]. Indeed, this is a further source of numerical uncertainty, which, however, is well under control.

- The agreement between the inverse Mellin transform of N -space time-like splitting functions and their x -space counterparts is also good, both at NLO and NNLO. Indeed, in figure 2 the relative difference between them is $\Delta P/P \lesssim 10^{-4}$, irrespective of the splitting function and the perturbative order. Note however that the value of $\Delta P/P$ is larger in figure 2 than in figure 1. In the former case, there is an additional uncertainty related to the numerical inverse Mellin transform of N -space splitting functions back to x space.

We conclude that the expressions of the splitting functions available in the literature are perfectly consistent with each other.³

3 Numerical implementation and benchmark

In this section, we present our implementation of time-like evolution in the $\overline{\text{MS}}$ factorisation scheme up to NNLO accuracy. The discussion is organised in three steps. First, we briefly discuss the numerical solution of DGLAP equations and their implementation in two different programs. Second, we define the setup conditions. Third, we present the results of a benchmark between our two codes.

³We would like to draw the reader’s attention on a couple of minor misprints that we came across in the literature during the checks we performed. In the `arXiv` version of ref. [42], there should be a minus sign, rather than a plus sign, in front of $\text{Li}_2(x)$ in the definition of $H(1, 0; x)$, eq. (11). In ref. [44], in the definition of $S_{-k}(N)$, second relation in eq. (10), the squared bracket should be closed before $\zeta(k)$, rather than after, see also eq. (46) of ref. [46]. Finally, a couple of misprints affecting both x - and N -space expressions of P^{qg} in ref. [31], eqs. (C.10) and (B.10) respectively, have been corrected in a revised version recently submitted to the `arXiv`.

3.1 The codes

We have implemented the time-like evolution in two entirely independent and conceptually different programs, based respectively on the solution of DGLAP equations (2.1)-(2.6) in x and N space. Provided perfectly controlled conditions, our goal is to obtain the same results irrespective of the procedure followed in the two codes. This provides a strong check of the correctness of both our implementations and our results.

As far as the x -space solution is concerned, we have implemented it in the already existing **APFEL** library [21]. Specifically, **APFEL** provides a framework in which the DGLAP equations are solved in x space by means of higher-order interpolation techniques, followed by the Runge-Kutta solution of the resulting discretised evolution equations. We refer the reader to ref. [21] for technical details on the implementation.

As far as the N -space solution is concerned, we have developed a new dedicated program: **MELA**, Mellin Evolution LibrAry. **MELA** exploits the fact that, in N space, the integro-differential DGLAP equations (2.1) are turned into the more simple ODEs (2.6). While eqs. (2.1) can be solved only by means of numerical methods, eqs. (2.6) allow for a simple analytical solution [47]. The numerical evaluation of the latter is immediate and, in principle, infinitely accurate. Of course, one should perform the numerical inversion of the solution from N space back to x space, but this is technically much easier than solving eq. (2.1) directly. In **MELA**, the inverse Mellin transform is performed by means of a numerical implementation of eq. (2.8) based on the Talbot-path algorithm [48].

Note that the solution of eqs. (2.6) requires the knowledge of the analytical expressions of the Mellin moments of the FFs over the whole complex plane. Hence, the parameterisation of FFs, usually given in x space, should be sufficiently simple to allow for an analytical Mellin transform. Of course, this greatly restricts the range of application of the N -space solution of the DGLAP equations. In order to bypass this limitation, the so-called **FastKernel** method [49], which allows one to evolve x -space distributions using the N -space approach by means of interpolation techniques, has been developed. This method has been implemented in **MELA** for completeness, even though this is not required by our study. Further investigations based on the extension of the **FastKernel** method to the time-like case will be left for future studies.

3.2 The setup

Our goal is to consistently compare **APFEL** and **MELA**. In order to do that, we need to choose a common setup for the evolution. Specifically, we use the following value of the strong coupling at the charm mass m_c :

$$\alpha_s(m_c) = 0.35, \quad (3.1)$$

and the following values for the heavy quark masses:

$$m_c = 1.43 \text{ GeV}, \quad m_b = 4.3 \text{ GeV}. \quad (3.2)$$

The top quark mass m_t does not need to be specified because the top-mass threshold will never be crossed in our computations.

We take the parameterisation for the initial-scale FFs from ref. [25]. In particular, we consider the π^+ FFs at NLO, eqs. (14)-(16), with the parameter values collected in table VI of ref. [25]

$$\begin{aligned}
D_u^{\pi^+}(x, \mu_0^2) &= D_d^{\pi^+}(x, \mu_0^2) = N_v^{\pi^+} x^{-0.963} (1-x)^{1.370}, \\
D_u^{\pi^+}(x, \mu_0^2) &= D_d^{\pi^+}(x, \mu_0^2) = D_s^{\pi^+}(x, \mu_0^2) = D_{\bar{s}}^{\pi^+}(x, \mu_0^2) = N_s^{\pi^+} x^{0.718} (1-x)^{6.266}, \\
D_g^{\pi^+}(x, \mu_0^2) &= N_g^{\pi^+} x^{1.943} (1-x)^8.
\end{aligned} \tag{3.3}$$

Here $\mu_0^2 = 1 \text{ GeV}^2$ and the normalisation constants $N_v^{\pi^+}$, $N_s^{\pi^+}$ and $N_g^{\pi^+}$ are such that

$$\int_0^1 dx x D_u^{\pi^+}(x, \mu_0^2) = 0.401, \quad \int_0^1 dx x D_s^{\pi^+}(x, \mu_0^2) = 0.094, \quad \int_0^1 dx x D_g^{\pi^+}(x, \mu_0^2) = 0.238. \tag{3.4}$$

Note that we consider only gluon and light quark FFs: indeed, in our programs heavy-quark components of FFs are dynamically generated at the corresponding thresholds. For this reason, they do not need to be parameterised. Consistently, we include matching conditions in the treatment of flavour threshold crossing in the evolution (2.1): in this respect, we note that, differently from PDFs, FFs undergo a non-zero matching at the heavy-quark thresholds already at NLO [50], while the matching at NNLO is presently unknown.

We would like to stress that the choice of the parameterisation given by eq. (3.3) is arbitrary. Essentially, this is motivated by its simplicity, which allowed us to easily obtain the corresponding analytic Mellin transform required by MELA. Therefore, this parameterisation should not be considered more reliable than any other, and the FFs given in eq. (3.3) should be regarded just as a set of test functions with some degree of realistic behaviour.

3.3 The results

The benchmark between APFEL and MELA is performed by comparing the result of the evolution of the set of FFs (3.3) for two different factorisation schemes, for different ratios between renormalisation and factorisation scales and at different final scales.

As far as the factorisation scheme is concerned, at NLO we consider two options: the Fixed-Flavour-Number Scheme (FFNS) with $n_f = 3$, in which the number of active flavours remains fixed and no heavy quark FF is generated during the evolution, and the Variable-Flavour-Number Scheme (VFNS), in which the heavy-quark FFs are dynamically generated as the evolution scale crosses the corresponding heavy-quark thresholds. The lack of knowledge on matching conditions prevents us to provide results in the VFNS at NNLO: hence, in this case, we perform the evolution only in the FFNS.

As a further cross-check, we also consider the more general case in which the factorisation scale μ_F , at which FFs are evaluated, and the renormalisation scale μ_R , at which α_s is evaluated, take different values ($\mu_F \neq \mu_R$). In this case, the effective splitting functions depend on the coefficients of the perturbative expansion of the QCD β -function and on



Figure 3: The ratio $R_{\text{MELA/APFEL}}(x) = D_{i,\text{MELA}}^{\pi^+}(x)/D_{i,\text{APFEL}}^{\pi^+}(x)$ for the comparison between the positive charged pion fragmentation functions of gluon, up, strange and charm quarks evolved at different values of μ_F^2 with **APFEL** and **MELA**. Results refer to different values of the ratio of the renormalisation and factorisation scales, μ_R^2/μ_F^2 , in the FFNS at NLO.

powers of $\ln(\mu_F^2/\mu_R^2)$ [47]. In addition, if $\mu_F \neq \mu_R$, the matching of α_s is no longer performed at the heavy-quark threshold, thus giving rise to discontinuities in the evolution of α_s . In our benchmark we consider three different values for the ratio μ_R^2/μ_F^2 : 1/2, 1, 2.

We evolve the set of FFs, eq. (3.3), from $\mu_0^2 = 1 \text{ GeV}^2$ to four different final scales, namely $\mu_F^2 = 10, 100, 1000, 10000 \text{ GeV}^2$. As for the momentum fraction, we look at the range $x \geq 0.01$, consistently with the kinematic cut usually imposed in global QCD analyses of FFs. Actually, beyond LO, time-like splitting functions have a much more singular behaviour than their space-like counterparts as $x \rightarrow 0$. Specifically, they present a double-logarithm enhancement with leading terms of the form $\alpha_s^n \ln^{2n-2} x$ (corresponding to poles of the form $\alpha_s^n (N-1)^{1-2n}$ in N space). Despite large cancellations between leading and non-leading logarithms at non-asymptotic values of x , the resulting small- x rise in the time-like case dwarfs that of the space-like case. This justifies the rather restricted range of momentum fractions we look at.

In figure 3, we show the ratio between gluon, up quark and strange quark FFs evolved at NLO with **APFEL** and **MELA** from $\mu_0^2 = 1 \text{ GeV}^2$ to $\mu_F^2 = 10, 100, 1000, 10000 \text{ GeV}^2$ for three different values of the ratio μ_R^2/μ_F^2 in the FFNS. In figure 4, we show the same comparison as in figure 3, but in the VFNS; here we display also the ratio for the charm quark FF, which is dynamically generated at the charm threshold. In figure 5, we show the same quantity as in figure 3, but at NNLO. All results are in the $\overline{\text{MS}}$ scheme.

Figures 3-4-5 show that the agreement between **APFEL** and **MELA** is optimal over all

APFEL vs. MELA: VFNS at NLO

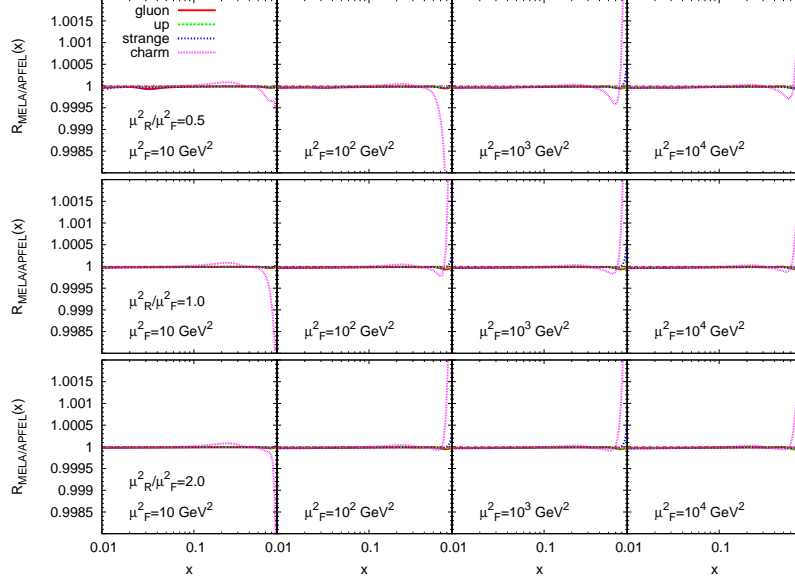


Figure 4: Same as figure 3, but in the VFNS.

APFEL vs. MELA: FFNS at NNLO



Figure 5: Same as figure 3, but at NNLO.

the (x, μ_F^2) region explored, the accuracy being below the 10^{-4} level. A slight worsening is observed only for the strange and charm quark FFs in the very large- x region. Here the absolute values of these distributions become extremely small and numerical effects start

coming in.

We conclude that proper implementations of both x - and N -space methods for the solution of the time-like DGLAP equations have been achieved in **APFEL** and **MELA** up to NNLO. The reliability of our results has been carefully checked step by step in order to exclude any inconsistency from the core of the evolution (splitting functions) up to the complete evolution mechanism. In order to facilitate a possible comparison with other codes, in appendix A we present a collection of tables reporting the numerical values of FFs at some reference values of x and μ_F^2 . The tables in appendix A, as well as the plots in figures 3-4-5, can be reproduced by running the benchmark suite of **MELA**, as explained in appendix B.

4 Conclusions and outlook

We have presented numerical results of the time-like evolution of FFs in the $\overline{\text{MS}}$ factorisation scheme for the first time up to NNLO accuracy in QCD. A high-precision comparison between x - and N -space solutions of the DGLAP evolution equations has been provided based on two entirely independent and conceptually different programs: **APFEL**, which has been updated for handling time-like evolution, and **MELA**, which has been specifically developed for the purpose of this paper.

This study has made us scrutinise the expressions of the time-like splitting functions available in the literature, in both x and N space. We have checked that all available results in the literature are mutually consistent.

We have obtained an excellent numerical agreement between **APFEL** and **MELA** results, achieving a relative accuracy well below 10^{-4} . The stability and reliability of the evolution codes has also been extensively tested upon various theoretical assumptions, including fixed- and variable-flavour number schemes and different factorisation and normalisation scale ratios. Above all, we managed to control the evolution of FFs at a level of accuracy which is comparable to that demanded for PDFs.

Our results aims at providing a reference for future global analyses of FFs; these may include a determination based on the NNPDF methodology [51, 52], thanks to the efficiency and flexibility of **APFEL**. In the future, we hope our results will be compared with other available codes, namely **QCDnum** and **ffevol**: this will call for a dedicated effort, which should benefit from the collaboration of the authors of these programs.

APFEL is available from its **HepForge** website:

<http://apfel.hepforge.org/>

MELA is available from:

<http://apfel.hepforge.org/mela.html>

We provide basic instructions for downloading and running it in appendix B.

Acknowledgments

We thank A. Mitov, S. Moch and A. Vogt for discussions about the results presented in this paper. We acknowledge S. Forte and J. Rojo for comments on the manuscript. This work is partially supported by an Italian PRIN2010 grant (S.C. and E.R.N.), by a European Investment Bank EIBURS grant (S.C.) and by the ERC grant 291377, LHCtheory: *Theoretical predictions and analyses of LHC physics: advancing the precision frontier* (V.B. and S.C.).

A Numerical Results

In this appendix, we present a collection of tables with the values of the FFs evolved as explained in section 3. We recall that we use the following values for the strong coupling at the charm mass m_c and the charm and bottom quark masses:

$$\alpha_s(m_c) = 0.35, \quad m_c = 1.43 \text{ GeV}, \quad m_b = 4.3 \text{ GeV}. \quad (\text{A.1})$$

The parameterisations for the initial-scale FFs are taken from ref. [25] with the parameter values collected in table VI in that reference.

The following tables are meant to be used for future comparisons with other computations. The values contained in the tables, as well as the comparison plots in figures 3-4-5, should be reproducible by running the MELA benchmark code as explained in appendix B.

B The MELA evolution code

MELA (Mellin Evolution LibrAry) is a N -space evolution program developed specifically for the computation presented in this paper. The aim of MELA is to provide a simple and user-friendly cross-check of the time-like x -space evolution available in APFEL since v2.3.0.

Download

The last stable release is MELA 1.0.0 and it is available from the **HepForge** website:

<http://apfel.hepforge.org/mela.html>

In order to download the latest version and decompress the code locally, open a terminal and execute the following commands:

```
wget http://apfel.hepforge.org/downloads/MELA-1.0.0.tar.gz
tar xvf MELA-1.0.0.tar.gz
```

Running the benchmark code

In order to produce the plots presented in section 3.3, as well as the benchmark tables presented in appendix A, execute the following commands:

```
cd ./MELA/usr/
./Benchmark.sh
```

x	$D_g^{\pi^+}(x, Q_0)$	$D_u^{\pi^+}(x, Q_0)$	$D_s^{\pi^+}(x, Q_0)$
$1.0 \cdot 10^{-02}$	$1.4028 \cdot 10^{-01}$	$7.5485 \cdot 10^{-01}$	$-6.7003 \cdot 10^{-02}$
$5.0 \cdot 10^{-02}$	$1.0215 \cdot 10^{+00}$	$1.2618 \cdot 10^{+00}$	$5.6882 \cdot 10^{-01}$
$1.0 \cdot 10^{-01}$	$9.6274 \cdot 10^{-01}$	$1.0816 \cdot 10^{+00}$	$5.4671 \cdot 10^{-01}$
$2.0 \cdot 10^{-01}$	$7.2835 \cdot 10^{-01}$	$7.4260 \cdot 10^{-01}$	$3.8267 \cdot 10^{-01}$
$3.0 \cdot 10^{-01}$	$4.0737 \cdot 10^{-01}$	$5.1131 \cdot 10^{-01}$	$2.1467 \cdot 10^{-01}$
$4.0 \cdot 10^{-01}$	$1.6711 \cdot 10^{-01}$	$3.5699 \cdot 10^{-01}$	$9.8314 \cdot 10^{-02}$
$5.0 \cdot 10^{-01}$	$4.9557 \cdot 10^{-02}$	$2.4692 \cdot 10^{-01}$	$3.5922 \cdot 10^{-02}$
$6.0 \cdot 10^{-01}$	$1.0252 \cdot 10^{-02}$	$1.6227 \cdot 10^{-01}$	$9.7576 \cdot 10^{-03}$
$7.0 \cdot 10^{-01}$	$1.5593 \cdot 10^{-03}$	$9.5732 \cdot 10^{-02}$	$1.6906 \cdot 10^{-03}$
$8.0 \cdot 10^{-01}$	$2.6359 \cdot 10^{-04}$	$4.5769 \cdot 10^{-02}$	$1.3035 \cdot 10^{-04}$
$9.0 \cdot 10^{-01}$	$3.9247 \cdot 10^{-05}$	$1.3028 \cdot 10^{-02}$	$1.3262 \cdot 10^{-06}$

Table 1: Numerical values of gluon, up and strange FFs evolved at NLO in the FFNS up to $\mu_F^2 = 10 \text{ GeV}^2$, $\mu_R^2/\mu_F^2 = 1/2$, $\alpha_s(\mu_F^2) = 0.2770096$.

x	$D_g^{\pi^+}(x, Q_0)$	$D_u^{\pi^+}(x, Q_0)$	$D_s^{\pi^+}(x, Q_0)$
$1.0 \cdot 10^{-02}$	$4.9764 \cdot 10^{-01}$	$9.7894 \cdot 10^{-01}$	$1.5823 \cdot 10^{-01}$
$5.0 \cdot 10^{-02}$	$8.6824 \cdot 10^{-01}$	$1.1681 \cdot 10^{+00}$	$4.7168 \cdot 10^{-01}$
$1.0 \cdot 10^{-01}$	$8.3316 \cdot 10^{-01}$	$1.0034 \cdot 10^{+00}$	$4.6351 \cdot 10^{-01}$
$2.0 \cdot 10^{-01}$	$6.7795 \cdot 10^{-01}$	$7.1424 \cdot 10^{-01}$	$3.5073 \cdot 10^{-01}$
$3.0 \cdot 10^{-01}$	$4.0174 \cdot 10^{-01}$	$5.0877 \cdot 10^{-01}$	$2.0860 \cdot 10^{-01}$
$4.0 \cdot 10^{-01}$	$1.7301 \cdot 10^{-01}$	$3.6378 \cdot 10^{-01}$	$9.9818 \cdot 10^{-02}$
$5.0 \cdot 10^{-01}$	$5.3680 \cdot 10^{-02}$	$2.5559 \cdot 10^{-01}$	$3.7734 \cdot 10^{-02}$
$6.0 \cdot 10^{-01}$	$1.1609 \cdot 10^{-02}$	$1.7010 \cdot 10^{-01}$	$1.0539 \cdot 10^{-02}$
$7.0 \cdot 10^{-01}$	$1.8188 \cdot 10^{-03}$	$1.0175 \cdot 10^{-01}$	$1.8733 \cdot 10^{-03}$
$8.0 \cdot 10^{-01}$	$2.9568 \cdot 10^{-04}$	$4.9561 \cdot 10^{-02}$	$1.4898 \cdot 10^{-04}$
$9.0 \cdot 10^{-01}$	$4.1078 \cdot 10^{-05}$	$1.4556 \cdot 10^{-02}$	$1.6551 \cdot 10^{-06}$

Table 2: Same as table 1: FFNS, $\mu_F^2 = 10 \text{ GeV}^2$, $\mu_R^2/\mu_F^2 = 1$, $\alpha_s(\mu_F^2) = 0.2393111$.

x	$D_g^{\pi^+}(x, Q_0)$	$D_u^{\pi^+}(x, Q_0)$	$D_s^{\pi^+}(x, Q_0)$
$1.0 \cdot 10^{-02}$	$5.8087 \cdot 10^{-01}$	$1.0412 \cdot 10^{+00}$	$2.2016 \cdot 10^{-01}$
$5.0 \cdot 10^{-02}$	$7.7199 \cdot 10^{-01}$	$1.1158 \cdot 10^{+00}$	$4.1428 \cdot 10^{-01}$
$1.0 \cdot 10^{-01}$	$7.6289 \cdot 10^{-01}$	$9.6544 \cdot 10^{-01}$	$4.1913 \cdot 10^{-01}$
$2.0 \cdot 10^{-01}$	$6.6472 \cdot 10^{-01}$	$7.0473 \cdot 10^{-01}$	$3.3668 \cdot 10^{-01}$
$3.0 \cdot 10^{-01}$	$4.1434 \cdot 10^{-01}$	$5.1305 \cdot 10^{-01}$	$2.0858 \cdot 10^{-01}$
$4.0 \cdot 10^{-01}$	$1.8581 \cdot 10^{-01}$	$3.7269 \cdot 10^{-01}$	$1.0285 \cdot 10^{-01}$
$5.0 \cdot 10^{-01}$	$5.9703 \cdot 10^{-02}$	$2.6492 \cdot 10^{-01}$	$3.9815 \cdot 10^{-02}$
$6.0 \cdot 10^{-01}$	$1.3277 \cdot 10^{-02}$	$1.7818 \cdot 10^{-01}$	$1.1349 \cdot 10^{-02}$
$7.0 \cdot 10^{-01}$	$2.0841 \cdot 10^{-03}$	$1.0788 \cdot 10^{-01}$	$2.0572 \cdot 10^{-03}$
$8.0 \cdot 10^{-01}$	$3.2211 \cdot 10^{-04}$	$5.3420 \cdot 10^{-02}$	$1.6750 \cdot 10^{-04}$
$9.0 \cdot 10^{-01}$	$4.3275 \cdot 10^{-05}$	$1.6124 \cdot 10^{-02}$	$1.9614 \cdot 10^{-06}$

Table 3: Same as table 1: FFNS, $\mu_F^2 = 10 \text{ GeV}^2$, $\mu_R^2/\mu_F^2 = 2$, $\alpha_s(\mu_F^2) = 0.2110517$.

x	$D_g^{\pi^+}(x, Q_0)$	$D_u^{\pi^+}(x, Q_0)$	$D_s^{\pi^+}(x, Q_0)$
$1.0 \cdot 10^{-02}$	$1.4340 \cdot 10^{+00}$	$1.3327 \cdot 10^{+00}$	$5.2393 \cdot 10^{-01}$
$5.0 \cdot 10^{-02}$	$1.4491 \cdot 10^{+00}$	$1.4809 \cdot 10^{+00}$	$8.3349 \cdot 10^{-01}$
$1.0 \cdot 10^{-01}$	$1.0512 \cdot 10^{+00}$	$1.1286 \cdot 10^{+00}$	$6.4251 \cdot 10^{-01}$
$2.0 \cdot 10^{-01}$	$5.5687 \cdot 10^{-01}$	$6.8324 \cdot 10^{-01}$	$3.5879 \cdot 10^{-01}$
$3.0 \cdot 10^{-01}$	$2.4010 \cdot 10^{-01}$	$4.3584 \cdot 10^{-01}$	$1.7432 \cdot 10^{-01}$
$4.0 \cdot 10^{-01}$	$8.0347 \cdot 10^{-02}$	$2.8747 \cdot 10^{-01}$	$7.1450 \cdot 10^{-02}$
$5.0 \cdot 10^{-01}$	$2.0548 \cdot 10^{-02}$	$1.8837 \cdot 10^{-01}$	$2.3713 \cdot 10^{-02}$
$6.0 \cdot 10^{-01}$	$4.1359 \cdot 10^{-03}$	$1.1647 \cdot 10^{-01}$	$5.8741 \cdot 10^{-03}$
$7.0 \cdot 10^{-01}$	$8.0031 \cdot 10^{-04}$	$6.3757 \cdot 10^{-02}$	$9.2263 \cdot 10^{-04}$
$8.0 \cdot 10^{-01}$	$1.7251 \cdot 10^{-04}$	$2.7544 \cdot 10^{-02}$	$6.3248 \cdot 10^{-05}$
$9.0 \cdot 10^{-01}$	$2.0689 \cdot 10^{-05}$	$6.6359 \cdot 10^{-03}$	$5.4430 \cdot 10^{-07}$

Table 4: Same as table 1: FFNS, $\mu_F^2 = 10^2 \text{ GeV}^2$, $\mu_R^2/\mu_F^2 = 1/2$, $\alpha_s(\mu_F^2) = 0.1829054$.

x	$D_g^{\pi^+}(x, Q_0)$	$D_u^{\pi^+}(x, Q_0)$	$D_s^{\pi^+}(x, Q_0)$
$1.0 \cdot 10^{-02}$	$1.5369 \cdot 10^{+00}$	$1.4617 \cdot 10^{+00}$	$6.5377 \cdot 10^{-01}$
$5.0 \cdot 10^{-02}$	$1.2399 \cdot 10^{+00}$	$1.3476 \cdot 10^{+00}$	$6.9561 \cdot 10^{-01}$
$1.0 \cdot 10^{-01}$	$9.2734 \cdot 10^{-01}$	$1.0438 \cdot 10^{+00}$	$5.5200 \cdot 10^{-01}$
$2.0 \cdot 10^{-01}$	$5.2786 \cdot 10^{-01}$	$6.6130 \cdot 10^{-01}$	$3.3263 \cdot 10^{-01}$
$3.0 \cdot 10^{-01}$	$2.4154 \cdot 10^{-01}$	$4.3762 \cdot 10^{-01}$	$1.7148 \cdot 10^{-01}$
$4.0 \cdot 10^{-01}$	$8.5126 \cdot 10^{-02}$	$2.9581 \cdot 10^{-01}$	$7.3565 \cdot 10^{-02}$
$5.0 \cdot 10^{-01}$	$2.2822 \cdot 10^{-02}$	$1.9707 \cdot 10^{-01}$	$2.5309 \cdot 10^{-02}$
$6.0 \cdot 10^{-01}$	$4.7668 \cdot 10^{-03}$	$1.2362 \cdot 10^{-01}$	$6.4603 \cdot 10^{-03}$
$7.0 \cdot 10^{-01}$	$9.2483 \cdot 10^{-04}$	$6.8785 \cdot 10^{-02}$	$1.0440 \cdot 10^{-03}$
$8.0 \cdot 10^{-01}$	$1.9406 \cdot 10^{-04}$	$3.0385 \cdot 10^{-02}$	$7.4134 \cdot 10^{-05}$
$9.0 \cdot 10^{-01}$	$2.2911 \cdot 10^{-05}$	$7.5963 \cdot 10^{-03}$	$7.0588 \cdot 10^{-07}$

Table 5: Same as table 1: FFNS, $\mu_F^2 = 10^2 \text{ GeV}^2$, $\mu_R^2/\mu_F^2 = 1$, $\alpha_s(\mu_F^2) = 0.1663143$.

x	$D_g^{\pi^+}(x, Q_0)$	$D_u^{\pi^+}(x, Q_0)$	$D_s^{\pi^+}(x, Q_0)$
$1.0 \cdot 10^{-02}$	$1.4844 \cdot 10^{+00}$	$1.4650 \cdot 10^{+00}$	$6.5605 \cdot 10^{-01}$
$5.0 \cdot 10^{-02}$	$1.1209 \cdot 10^{+00}$	$1.2757 \cdot 10^{+00}$	$6.1705 \cdot 10^{-01}$
$1.0 \cdot 10^{-01}$	$8.6823 \cdot 10^{-01}$	$1.0045 \cdot 10^{+00}$	$5.0518 \cdot 10^{-01}$
$2.0 \cdot 10^{-01}$	$5.2896 \cdot 10^{-01}$	$6.5723 \cdot 10^{-01}$	$3.2305 \cdot 10^{-01}$
$3.0 \cdot 10^{-01}$	$2.5532 \cdot 10^{-01}$	$4.4560 \cdot 10^{-01}$	$1.7382 \cdot 10^{-01}$
$4.0 \cdot 10^{-01}$	$9.4016 \cdot 10^{-02}$	$3.0637 \cdot 10^{-01}$	$7.7023 \cdot 10^{-02}$
$5.0 \cdot 10^{-01}$	$2.6112 \cdot 10^{-02}$	$2.0682 \cdot 10^{-01}$	$2.7204 \cdot 10^{-02}$
$6.0 \cdot 10^{-01}$	$5.5517 \cdot 10^{-03}$	$1.3142 \cdot 10^{-01}$	$7.1061 \cdot 10^{-03}$
$7.0 \cdot 10^{-01}$	$1.0569 \cdot 10^{-03}$	$7.4243 \cdot 10^{-02}$	$1.1750 \cdot 10^{-03}$
$8.0 \cdot 10^{-01}$	$2.1577 \cdot 10^{-04}$	$3.3477 \cdot 10^{-02}$	$8.5823 \cdot 10^{-05}$
$9.0 \cdot 10^{-01}$	$2.5554 \cdot 10^{-05}$	$8.6589 \cdot 10^{-03}$	$8.6990 \cdot 10^{-07}$

Table 6: Same as table 1: FFNS, $\mu_F^2 = 10^2 \text{ GeV}^2$, $\mu_R^2/\mu_F^2 = 2$, $\alpha_s(\mu_F^2) = 0.1525814$.

x	$D_g^{\pi^+}(x, Q_0)$	$D_u^{\pi^+}(x, Q_0)$	$D_s^{\pi^+}(x, Q_0)$
$1.0 \cdot 10^{-02}$	$2.5036 \cdot 10^{+00}$	$1.8809 \cdot 10^{+00}$	$1.0840 \cdot 10^{+00}$
$5.0 \cdot 10^{-02}$	$1.6021 \cdot 10^{+00}$	$1.5851 \cdot 10^{+00}$	$9.7056 \cdot 10^{-01}$
$1.0 \cdot 10^{-01}$	$1.0000 \cdot 10^{+00}$	$1.1182 \cdot 10^{+00}$	$6.6513 \cdot 10^{-01}$
$2.0 \cdot 10^{-01}$	$4.2870 \cdot 10^{-01}$	$6.2699 \cdot 10^{-01}$	$3.2715 \cdot 10^{-01}$
$3.0 \cdot 10^{-01}$	$1.5797 \cdot 10^{-01}$	$3.8269 \cdot 10^{-01}$	$1.4614 \cdot 10^{-01}$
$4.0 \cdot 10^{-01}$	$4.7042 \cdot 10^{-02}$	$2.4375 \cdot 10^{-01}$	$5.6016 \cdot 10^{-02}$
$5.0 \cdot 10^{-01}$	$1.1332 \cdot 10^{-02}$	$1.5400 \cdot 10^{-01}$	$1.7502 \cdot 10^{-02}$
$6.0 \cdot 10^{-01}$	$2.4107 \cdot 10^{-03}$	$9.1246 \cdot 10^{-02}$	$4.0827 \cdot 10^{-03}$
$7.0 \cdot 10^{-01}$	$5.4799 \cdot 10^{-04}$	$4.7376 \cdot 10^{-02}$	$6.0057 \cdot 10^{-04}$
$8.0 \cdot 10^{-01}$	$1.2080 \cdot 10^{-04}$	$1.9061 \cdot 10^{-02}$	$3.8052 \cdot 10^{-05}$
$9.0 \cdot 10^{-01}$	$1.2251 \cdot 10^{-05}$	$4.0856 \cdot 10^{-03}$	$2.9598 \cdot 10^{-07}$

Table 7: Same as table 1: FFNS, $\mu_F^2 = 10^3 \text{ GeV}^2$, $\mu_R^2/\mu_F^2 = 1/2$, $\alpha_s(\mu_F^2) = 0.1376668$.

x	$D_g^{\pi^+}(x, Q_0)$	$D_u^{\pi^+}(x, Q_0)$	$D_s^{\pi^+}(x, Q_0)$
$1.0 \cdot 10^{-02}$	$2.3917 \cdot 10^{+00}$	$1.9100 \cdot 10^{+00}$	$1.1136 \cdot 10^{+00}$
$5.0 \cdot 10^{-02}$	$1.3868 \cdot 10^{+00}$	$1.4381 \cdot 10^{+00}$	$8.1858 \cdot 10^{-01}$
$1.0 \cdot 10^{-01}$	$8.9640 \cdot 10^{-01}$	$1.0374 \cdot 10^{+00}$	$5.7848 \cdot 10^{-01}$
$2.0 \cdot 10^{-01}$	$4.1235 \cdot 10^{-01}$	$6.1053 \cdot 10^{-01}$	$3.0621 \cdot 10^{-01}$
$3.0 \cdot 10^{-01}$	$1.6110 \cdot 10^{-01}$	$3.8654 \cdot 10^{-01}$	$1.4496 \cdot 10^{-01}$
$4.0 \cdot 10^{-01}$	$5.0482 \cdot 10^{-02}$	$2.5217 \cdot 10^{-01}$	$5.8119 \cdot 10^{-02}$
$5.0 \cdot 10^{-01}$	$1.2699 \cdot 10^{-02}$	$1.6199 \cdot 10^{-01}$	$1.8821 \cdot 10^{-02}$
$6.0 \cdot 10^{-01}$	$2.7690 \cdot 10^{-03}$	$9.7429 \cdot 10^{-02}$	$4.5254 \cdot 10^{-03}$
$7.0 \cdot 10^{-01}$	$6.2571 \cdot 10^{-04}$	$5.1475 \cdot 10^{-02}$	$6.8541 \cdot 10^{-04}$
$8.0 \cdot 10^{-01}$	$1.3653 \cdot 10^{-04}$	$2.1204 \cdot 10^{-02}$	$4.5049 \cdot 10^{-05}$
$9.0 \cdot 10^{-01}$	$1.3932 \cdot 10^{-05}$	$4.7266 \cdot 10^{-03}$	$3.8945 \cdot 10^{-07}$

Table 8: Same as table 1: FFNS, $\mu_F^2 = 10^3 \text{ GeV}^2$, $\mu_R^2/\mu_F^2 = 1$, $\alpha_s(\mu_F^2) = 0.1282435$.

x	$D_g^{\pi^+}(x, Q_0)$	$D_u^{\pi^+}(x, Q_0)$	$D_s^{\pi^+}(x, Q_0)$
$1.0 \cdot 10^{-02}$	$2.2362 \cdot 10^{+00}$	$1.8597 \cdot 10^{+00}$	$1.0617 \cdot 10^{+00}$
$5.0 \cdot 10^{-02}$	$1.2724 \cdot 10^{+00}$	$1.3614 \cdot 10^{+00}$	$7.3454 \cdot 10^{-01}$
$1.0 \cdot 10^{-01}$	$8.5344 \cdot 10^{-01}$	$1.0021 \cdot 10^{+00}$	$5.3545 \cdot 10^{-01}$
$2.0 \cdot 10^{-01}$	$4.1952 \cdot 10^{-01}$	$6.1030 \cdot 10^{-01}$	$3.0014 \cdot 10^{-01}$
$3.0 \cdot 10^{-01}$	$1.7273 \cdot 10^{-01}$	$3.9591 \cdot 10^{-01}$	$1.4819 \cdot 10^{-01}$
$4.0 \cdot 10^{-01}$	$5.6467 \cdot 10^{-02}$	$2.6272 \cdot 10^{-01}$	$6.1368 \cdot 10^{-02}$
$5.0 \cdot 10^{-01}$	$1.4636 \cdot 10^{-02}$	$1.7110 \cdot 10^{-01}$	$2.0409 \cdot 10^{-02}$
$6.0 \cdot 10^{-01}$	$3.2091 \cdot 10^{-03}$	$1.0434 \cdot 10^{-01}$	$5.0254 \cdot 10^{-03}$
$7.0 \cdot 10^{-01}$	$7.1001 \cdot 10^{-04}$	$5.6041 \cdot 10^{-02}$	$7.7970 \cdot 10^{-04}$
$8.0 \cdot 10^{-01}$	$1.5362 \cdot 10^{-04}$	$2.3605 \cdot 10^{-02}$	$5.2800 \cdot 10^{-05}$
$9.0 \cdot 10^{-01}$	$1.5949 \cdot 10^{-05}$	$5.4590 \cdot 10^{-03}$	$4.8763 \cdot 10^{-07}$

Table 9: Same as table 1: FFNS, $\mu_F^2 = 10^3 \text{ GeV}^2$, $\mu_R^2/\mu_F^2 = 2$, $\alpha_s(\mu_F^2) = 0.1200632$.

x	$D_g^{\pi^+}(x, Q_0)$	$D_u^{\pi^+}(x, Q_0)$	$D_s^{\pi^+}(x, Q_0)$
$1.0 \cdot 10^{-02}$	$3.3009 \cdot 10^{+00}$	$2.3350 \cdot 10^{+00}$	$1.5488 \cdot 10^{+00}$
$5.0 \cdot 10^{-02}$	$1.6386 \cdot 10^{+00}$	$1.6340 \cdot 10^{+00}$	$1.0451 \cdot 10^{+00}$
$1.0 \cdot 10^{-01}$	$9.2041 \cdot 10^{-01}$	$1.0909 \cdot 10^{+00}$	$6.6264 \cdot 10^{-01}$
$2.0 \cdot 10^{-01}$	$3.3987 \cdot 10^{-01}$	$5.8002 \cdot 10^{-01}$	$2.9899 \cdot 10^{-01}$
$3.0 \cdot 10^{-01}$	$1.1232 \cdot 10^{-01}$	$3.4342 \cdot 10^{-01}$	$1.2597 \cdot 10^{-01}$
$4.0 \cdot 10^{-01}$	$3.1092 \cdot 10^{-02}$	$2.1320 \cdot 10^{-01}$	$4.6024 \cdot 10^{-02}$
$5.0 \cdot 10^{-01}$	$7.3648 \cdot 10^{-03}$	$1.3097 \cdot 10^{-01}$	$1.3757 \cdot 10^{-02}$
$6.0 \cdot 10^{-01}$	$1.6806 \cdot 10^{-03}$	$7.5057 \cdot 10^{-02}$	$3.0681 \cdot 10^{-03}$
$7.0 \cdot 10^{-01}$	$4.1621 \cdot 10^{-04}$	$3.7400 \cdot 10^{-02}$	$4.2947 \cdot 10^{-04}$
$8.0 \cdot 10^{-01}$	$8.9420 \cdot 10^{-05}$	$1.4237 \cdot 10^{-02}$	$2.5637 \cdot 10^{-05}$
$9.0 \cdot 10^{-01}$	$7.9956 \cdot 10^{-06}$	$2.7874 \cdot 10^{-03}$	$1.8560 \cdot 10^{-07}$

Table 10: Same as table 1: FFNS, $\mu_F^2 = 10^4 \text{ GeV}^2$, $\mu_R^2/\mu_F^2 = 1/2$, $\alpha_s(\mu_F^2) = 0.1107665$.

x	$D_g^{\pi^+}(x, Q_0)$	$D_u^{\pi^+}(x, Q_0)$	$D_s^{\pi^+}(x, Q_0)$
$1.0 \cdot 10^{-02}$	$3.0377 \cdot 10^{+00}$	$2.2835 \cdot 10^{+00}$	$1.4974 \cdot 10^{+00}$
$5.0 \cdot 10^{-02}$	$1.4327 \cdot 10^{+00}$	$1.4831 \cdot 10^{+00}$	$8.8904 \cdot 10^{-01}$
$1.0 \cdot 10^{-01}$	$8.3511 \cdot 10^{-01}$	$1.0157 \cdot 10^{+00}$	$5.8162 \cdot 10^{-01}$
$2.0 \cdot 10^{-01}$	$3.3048 \cdot 10^{-01}$	$5.6746 \cdot 10^{-01}$	$2.8183 \cdot 10^{-01}$
$3.0 \cdot 10^{-01}$	$1.1566 \cdot 10^{-01}$	$3.4830 \cdot 10^{-01}$	$1.2567 \cdot 10^{-01}$
$4.0 \cdot 10^{-01}$	$3.3622 \cdot 10^{-02}$	$2.2133 \cdot 10^{-01}$	$4.7988 \cdot 10^{-02}$
$5.0 \cdot 10^{-01}$	$8.2715 \cdot 10^{-03}$	$1.3823 \cdot 10^{-01}$	$1.4861 \cdot 10^{-02}$
$6.0 \cdot 10^{-01}$	$1.9166 \cdot 10^{-03}$	$8.0443 \cdot 10^{-02}$	$3.4158 \cdot 10^{-03}$
$7.0 \cdot 10^{-01}$	$4.7207 \cdot 10^{-04}$	$4.0809 \cdot 10^{-02}$	$4.9242 \cdot 10^{-04}$
$8.0 \cdot 10^{-01}$	$1.0146 \cdot 10^{-04}$	$1.5917 \cdot 10^{-02}$	$3.0513 \cdot 10^{-05}$
$9.0 \cdot 10^{-01}$	$9.2326 \cdot 10^{-06}$	$3.2443 \cdot 10^{-03}$	$2.4600 \cdot 10^{-07}$

Table 11: Same as table 1: FFNS, $\mu_F^2 = 10^4 \text{ GeV}^2$, $\mu_R^2/\mu_F^2 = 1$, $\alpha_s(\mu_F^2) = 0.1046608$.

x	$D_g^{\pi^+}(x, Q_0)$	$D_u^{\pi^+}(x, Q_0)$	$D_s^{\pi^+}(x, Q_0)$
$1.0 \cdot 10^{-02}$	$2.8153 \cdot 10^{+00}$	$2.1928 \cdot 10^{+00}$	$1.4047 \cdot 10^{+00}$
$5.0 \cdot 10^{-02}$	$1.3296 \cdot 10^{+00}$	$1.4068 \cdot 10^{+00}$	$8.0505 \cdot 10^{-01}$
$1.0 \cdot 10^{-01}$	$8.0483 \cdot 10^{-01}$	$9.8487 \cdot 10^{-01}$	$5.4299 \cdot 10^{-01}$
$2.0 \cdot 10^{-01}$	$3.3981 \cdot 10^{-01}$	$5.6968 \cdot 10^{-01}$	$2.7806 \cdot 10^{-01}$
$3.0 \cdot 10^{-01}$	$1.2511 \cdot 10^{-01}$	$3.5815 \cdot 10^{-01}$	$1.2919 \cdot 10^{-01}$
$4.0 \cdot 10^{-01}$	$3.7830 \cdot 10^{-02}$	$2.3146 \cdot 10^{-01}$	$5.0935 \cdot 10^{-02}$
$5.0 \cdot 10^{-01}$	$9.5276 \cdot 10^{-03}$	$1.4659 \cdot 10^{-01}$	$1.6198 \cdot 10^{-02}$
$6.0 \cdot 10^{-01}$	$2.2022 \cdot 10^{-03}$	$8.6536 \cdot 10^{-02}$	$3.8135 \cdot 10^{-03}$
$7.0 \cdot 10^{-01}$	$5.3375 \cdot 10^{-04}$	$4.4661 \cdot 10^{-02}$	$5.6342 \cdot 10^{-04}$
$8.0 \cdot 10^{-01}$	$1.1502 \cdot 10^{-04}$	$1.7827 \cdot 10^{-02}$	$3.6000 \cdot 10^{-05}$
$9.0 \cdot 10^{-01}$	$1.0725 \cdot 10^{-05}$	$3.7752 \cdot 10^{-03}$	$3.1055 \cdot 10^{-07}$

Table 12: Same as table 1: FFNS, $\mu_F^2 = 10^4 \text{ GeV}^2$, $\mu_R^2/\mu_F^2 = 2$, $\alpha_s(\mu_F^2) = 0.0992090$.

x	$D_g^{\pi^+}(x, Q_0)$	$D_u^{\pi^+}(x, Q_0)$	$D_s^{\pi^+}(x, Q_0)$	$D_c^{\pi^+}(x, Q_0)$
$1.0 \cdot 10^{-02}$	$1.5492 \cdot 10^{-01}$	$7.6121 \cdot 10^{-01}$	$-6.0682 \cdot 10^{-02}$	$5.7231 \cdot 10^{-01}$
$5.0 \cdot 10^{-02}$	$9.9725 \cdot 10^{-01}$	$1.2571 \cdot 10^{+00}$	$5.6325 \cdot 10^{-01}$	$4.0424 \cdot 10^{-01}$
$1.0 \cdot 10^{-01}$	$9.4191 \cdot 10^{-01}$	$1.0792 \cdot 10^{+00}$	$5.4321 \cdot 10^{-01}$	$2.2772 \cdot 10^{-01}$
$2.0 \cdot 10^{-01}$	$7.1834 \cdot 10^{-01}$	$7.4315 \cdot 10^{-01}$	$3.8246 \cdot 10^{-01}$	$7.7980 \cdot 10^{-02}$
$3.0 \cdot 10^{-01}$	$4.0469 \cdot 10^{-01}$	$5.1287 \cdot 10^{-01}$	$2.1550 \cdot 10^{-01}$	$2.3808 \cdot 10^{-02}$
$4.0 \cdot 10^{-01}$	$1.6712 \cdot 10^{-01}$	$3.5872 \cdot 10^{-01}$	$9.9051 \cdot 10^{-02}$	$5.7948 \cdot 10^{-03}$
$5.0 \cdot 10^{-01}$	$4.9921 \cdot 10^{-02}$	$2.4851 \cdot 10^{-01}$	$3.6305 \cdot 10^{-02}$	$1.0162 \cdot 10^{-03}$
$6.0 \cdot 10^{-01}$	$1.0434 \cdot 10^{-02}$	$1.6359 \cdot 10^{-01}$	$9.8915 \cdot 10^{-03}$	$1.0678 \cdot 10^{-04}$
$7.0 \cdot 10^{-01}$	$1.6197 \cdot 10^{-03}$	$9.6718 \cdot 10^{-02}$	$1.7194 \cdot 10^{-03}$	$3.1017 \cdot 10^{-06}$
$8.0 \cdot 10^{-01}$	$2.8162 \cdot 10^{-04}$	$4.6376 \cdot 10^{-02}$	$1.3318 \cdot 10^{-04}$	$-5.5107 \cdot 10^{-07}$
$9.0 \cdot 10^{-01}$	$4.2458 \cdot 10^{-05}$	$1.3267 \cdot 10^{-02}$	$1.3727 \cdot 10^{-06}$	$-5.6280 \cdot 10^{-08}$

Table 13: Numerical values of gluon, up, strange and charm FFs evolved at NLO in the VFNS up to $\mu_F^2 = 10 \text{ GeV}^2$, $\mu_R^2/\mu_F^2 = 1/2$, $\alpha_s(\mu_F^2) = 0.2823897$.

x	$D_g^{\pi^+}(x, Q_0)$	$D_u^{\pi^+}(x, Q_0)$	$D_s^{\pi^+}(x, Q_0)$	$D_c^{\pi^+}(x, Q_0)$
$1.0 \cdot 10^{-02}$	$4.9673 \cdot 10^{-01}$	$9.7661 \cdot 10^{-01}$	$1.5592 \cdot 10^{-01}$	$5.4015 \cdot 10^{-01}$
$5.0 \cdot 10^{-02}$	$8.5963 \cdot 10^{-01}$	$1.1707 \cdot 10^{+00}$	$4.7431 \cdot 10^{-01}$	$3.2641 \cdot 10^{-01}$
$1.0 \cdot 10^{-01}$	$8.2220 \cdot 10^{-01}$	$1.0056 \cdot 10^{+00}$	$4.6563 \cdot 10^{-01}$	$1.8456 \cdot 10^{-01}$
$2.0 \cdot 10^{-01}$	$6.6765 \cdot 10^{-01}$	$7.1528 \cdot 10^{-01}$	$3.5174 \cdot 10^{-01}$	$6.5025 \cdot 10^{-02}$
$3.0 \cdot 10^{-01}$	$3.9549 \cdot 10^{-01}$	$5.0920 \cdot 10^{-01}$	$2.0901 \cdot 10^{-01}$	$2.0567 \cdot 10^{-02}$
$4.0 \cdot 10^{-01}$	$1.7037 \cdot 10^{-01}$	$3.6397 \cdot 10^{-01}$	$9.9961 \cdot 10^{-02}$	$5.2242 \cdot 10^{-03}$
$5.0 \cdot 10^{-01}$	$5.2930 \cdot 10^{-02}$	$2.5570 \cdot 10^{-01}$	$3.7780 \cdot 10^{-02}$	$9.7238 \cdot 10^{-04}$
$6.0 \cdot 10^{-01}$	$1.1495 \cdot 10^{-02}$	$1.7018 \cdot 10^{-01}$	$1.0552 \cdot 10^{-02}$	$1.1505 \cdot 10^{-04}$
$7.0 \cdot 10^{-01}$	$1.8275 \cdot 10^{-03}$	$1.0181 \cdot 10^{-01}$	$1.8759 \cdot 10^{-03}$	$6.2394 \cdot 10^{-06}$
$8.0 \cdot 10^{-01}$	$3.0556 \cdot 10^{-04}$	$4.9605 \cdot 10^{-02}$	$1.4927 \cdot 10^{-04}$	$-9.4928 \cdot 10^{-08}$
$9.0 \cdot 10^{-01}$	$4.3179 \cdot 10^{-05}$	$1.4576 \cdot 10^{-02}$	$1.6624 \cdot 10^{-06}$	$-2.8984 \cdot 10^{-08}$

Table 14: Same as table 13: VFNS, $\mu_F^2 = 10 \text{ GeV}^2$, $\mu_R^2/\mu_F^2 = 1$, $\alpha_s(\mu_F^2) = 0.2462915$.

x	$D_g^{\pi^+}(x, Q_0)$	$D_u^{\pi^+}(x, Q_0)$	$D_s^{\pi^+}(x, Q_0)$	$D_c^{\pi^+}(x, Q_0)$
$1.0 \cdot 10^{-02}$	$5.7877 \cdot 10^{-01}$	$1.0392 \cdot 10^{+00}$	$2.1814 \cdot 10^{-01}$	$4.8959 \cdot 10^{-01}$
$5.0 \cdot 10^{-02}$	$7.6567 \cdot 10^{-01}$	$1.1185 \cdot 10^{+00}$	$4.1713 \cdot 10^{-01}$	$2.7920 \cdot 10^{-01}$
$1.0 \cdot 10^{-01}$	$7.5334 \cdot 10^{-01}$	$9.6745 \cdot 10^{-01}$	$4.2134 \cdot 10^{-01}$	$1.5958 \cdot 10^{-01}$
$2.0 \cdot 10^{-01}$	$6.5368 \cdot 10^{-01}$	$7.0543 \cdot 10^{-01}$	$3.3752 \cdot 10^{-01}$	$5.7924 \cdot 10^{-02}$
$3.0 \cdot 10^{-01}$	$4.0666 \cdot 10^{-01}$	$5.1309 \cdot 10^{-01}$	$2.0876 \cdot 10^{-01}$	$1.8923 \cdot 10^{-02}$
$4.0 \cdot 10^{-01}$	$1.8218 \cdot 10^{-01}$	$3.7249 \cdot 10^{-01}$	$1.0282 \cdot 10^{-01}$	$4.9812 \cdot 10^{-03}$
$5.0 \cdot 10^{-01}$	$5.8534 \cdot 10^{-02}$	$2.6468 \cdot 10^{-01}$	$3.9775 \cdot 10^{-02}$	$9.6878 \cdot 10^{-04}$
$6.0 \cdot 10^{-01}$	$1.3048 \cdot 10^{-02}$	$1.7797 \cdot 10^{-01}$	$1.1331 \cdot 10^{-02}$	$1.2288 \cdot 10^{-04}$
$7.0 \cdot 10^{-01}$	$2.0712 \cdot 10^{-03}$	$1.0773 \cdot 10^{-01}$	$2.0532 \cdot 10^{-03}$	$8.1636 \cdot 10^{-06}$
$8.0 \cdot 10^{-01}$	$3.2831 \cdot 10^{-04}$	$5.3326 \cdot 10^{-02}$	$1.6712 \cdot 10^{-04}$	$1.6326 \cdot 10^{-07}$
$9.0 \cdot 10^{-01}$	$4.4872 \cdot 10^{-05}$	$1.6088 \cdot 10^{-02}$	$1.9574 \cdot 10^{-06}$	$-1.2078 \cdot 10^{-08}$

Table 15: Same as table 13: VFNS, $\mu_F^2 = 10 \text{ GeV}^2$, $\mu_R^2/\mu_F^2 = 2$, $\alpha_s(\mu_F^2) = 0.2179093$.

x	$D_g^{\pi^+}(x, Q_0)$	$D_u^{\pi^+}(x, Q_0)$	$D_s^{\pi^+}(x, Q_0)$	$D_c^{\pi^+}(x, Q_0)$
$1.0 \cdot 10^{-02}$	$1.4392 \cdot 10^{+00}$	$1.3449 \cdot 10^{+00}$	$5.3639 \cdot 10^{-01}$	$1.0538 \cdot 10^{+00}$
$5.0 \cdot 10^{-02}$	$1.3984 \cdot 10^{+00}$	$1.4810 \cdot 10^{+00}$	$8.3370 \cdot 10^{-01}$	$6.4282 \cdot 10^{-01}$
$1.0 \cdot 10^{-01}$	$1.0075 \cdot 10^{+00}$	$1.1281 \cdot 10^{+00}$	$6.4203 \cdot 10^{-01}$	$3.3614 \cdot 10^{-01}$
$2.0 \cdot 10^{-01}$	$5.3182 \cdot 10^{-01}$	$6.8312 \cdot 10^{-01}$	$3.5870 \cdot 10^{-01}$	$1.0195 \cdot 10^{-01}$
$3.0 \cdot 10^{-01}$	$2.2943 \cdot 10^{-01}$	$4.3596 \cdot 10^{-01}$	$1.7444 \cdot 10^{-01}$	$2.7940 \cdot 10^{-02}$
$4.0 \cdot 10^{-01}$	$7.7030 \cdot 10^{-02}$	$2.8767 \cdot 10^{-01}$	$7.1576 \cdot 10^{-02}$	$6.1888 \cdot 10^{-03}$
$5.0 \cdot 10^{-01}$	$1.9870 \cdot 10^{-02}$	$1.8857 \cdot 10^{-01}$	$2.3781 \cdot 10^{-02}$	$1.0124 \cdot 10^{-03}$
$6.0 \cdot 10^{-01}$	$4.0894 \cdot 10^{-03}$	$1.1666 \cdot 10^{-01}$	$5.8981 \cdot 10^{-03}$	$1.0872 \cdot 10^{-04}$
$7.0 \cdot 10^{-01}$	$8.2563 \cdot 10^{-04}$	$6.3903 \cdot 10^{-02}$	$9.2798 \cdot 10^{-04}$	$6.8820 \cdot 10^{-06}$
$8.0 \cdot 10^{-01}$	$1.8409 \cdot 10^{-04}$	$2.7637 \cdot 10^{-02}$	$6.3832 \cdot 10^{-05}$	$3.3464 \cdot 10^{-07}$
$9.0 \cdot 10^{-01}$	$2.2470 \cdot 10^{-05}$	$6.6713 \cdot 10^{-03}$	$5.5920 \cdot 10^{-07}$	$-3.5677 \cdot 10^{-10}$

Table 16: Same as table 13: VFNS, $\mu_F^2 = 10^2 \text{ GeV}^2$, $\mu_R^2/\mu_F^2 = 1/2$, $\alpha_s(\mu_F^2) = 0.1938346$.

x	$D_g^{\pi^+}(x, Q_0)$	$D_u^{\pi^+}(x, Q_0)$	$D_s^{\pi^+}(x, Q_0)$	$D_c^{\pi^+}(x, Q_0)$
$1.0 \cdot 10^{-02}$	$1.5355 \cdot 10^{+00}$	$1.4712 \cdot 10^{+00}$	$6.6365 \cdot 10^{-01}$	$9.7376 \cdot 10^{-01}$
$5.0 \cdot 10^{-02}$	$1.2070 \cdot 10^{+00}$	$1.3548 \cdot 10^{+00}$	$7.0408 \cdot 10^{-01}$	$5.3020 \cdot 10^{-01}$
$1.0 \cdot 10^{-01}$	$8.9152 \cdot 10^{-01}$	$1.0465 \cdot 10^{+00}$	$5.5597 \cdot 10^{-01}$	$2.8080 \cdot 10^{-01}$
$2.0 \cdot 10^{-01}$	$5.0053 \cdot 10^{-01}$	$6.6057 \cdot 10^{-01}$	$3.3280 \cdot 10^{-01}$	$8.8346 \cdot 10^{-02}$
$3.0 \cdot 10^{-01}$	$2.2730 \cdot 10^{-01}$	$4.3605 \cdot 10^{-01}$	$1.7082 \cdot 10^{-01}$	$2.5184 \cdot 10^{-02}$
$4.0 \cdot 10^{-01}$	$7.9809 \cdot 10^{-02}$	$2.9423 \cdot 10^{-01}$	$7.3049 \cdot 10^{-02}$	$5.8344 \cdot 10^{-03}$
$5.0 \cdot 10^{-01}$	$2.1440 \cdot 10^{-02}$	$1.9573 \cdot 10^{-01}$	$2.5068 \cdot 10^{-02}$	$1.0131 \cdot 10^{-03}$
$6.0 \cdot 10^{-01}$	$4.5498 \cdot 10^{-03}$	$1.2260 \cdot 10^{-01}$	$6.3849 \cdot 10^{-03}$	$1.2059 \cdot 10^{-04}$
$7.0 \cdot 10^{-01}$	$9.1769 \cdot 10^{-04}$	$6.8098 \cdot 10^{-02}$	$1.0297 \cdot 10^{-03}$	$9.6284 \cdot 10^{-06}$
$8.0 \cdot 10^{-01}$	$1.9945 \cdot 10^{-04}$	$3.0013 \cdot 10^{-02}$	$7.3001 \cdot 10^{-05}$	$6.6294 \cdot 10^{-07}$
$9.0 \cdot 10^{-01}$	$2.3977 \cdot 10^{-05}$	$7.4764 \cdot 10^{-03}$	$6.9708 \cdot 10^{-07}$	$1.5982 \cdot 10^{-08}$

Table 17: Same as table 13: VFNS, $\mu_F^2 = 10^2 \text{ GeV}^2$, $\mu_R^2/\mu_F^2 = 1$, $\alpha_s(\mu_F^2) = 0.1777432$.

x	$D_g^{\pi^+}(x, Q_0)$	$D_u^{\pi^+}(x, Q_0)$	$D_s^{\pi^+}(x, Q_0)$	$D_c^{\pi^+}(x, Q_0)$
$1.0 \cdot 10^{-02}$	$1.4786 \cdot 10^{+00}$	$1.4728 \cdot 10^{+00}$	$6.6434 \cdot 10^{-01}$	$8.8195 \cdot 10^{-01}$
$5.0 \cdot 10^{-02}$	$1.0919 \cdot 10^{+00}$	$1.2820 \cdot 10^{+00}$	$6.2492 \cdot 10^{-01}$	$4.6372 \cdot 10^{-01}$
$1.0 \cdot 10^{-01}$	$8.3428 \cdot 10^{-01}$	$1.0066 \cdot 10^{+00}$	$5.0888 \cdot 10^{-01}$	$2.5032 \cdot 10^{-01}$
$2.0 \cdot 10^{-01}$	$5.0011 \cdot 10^{-01}$	$6.5597 \cdot 10^{-01}$	$3.2292 \cdot 10^{-01}$	$8.1847 \cdot 10^{-02}$
$3.0 \cdot 10^{-01}$	$2.3909 \cdot 10^{-01}$	$4.4351 \cdot 10^{-01}$	$1.7285 \cdot 10^{-01}$	$2.4214 \cdot 10^{-02}$
$4.0 \cdot 10^{-01}$	$8.7547 \cdot 10^{-02}$	$3.0431 \cdot 10^{-01}$	$7.6299 \cdot 10^{-02}$	$5.8296 \cdot 10^{-03}$
$5.0 \cdot 10^{-01}$	$2.4307 \cdot 10^{-02}$	$2.0505 \cdot 10^{-01}$	$2.6862 \cdot 10^{-02}$	$1.0577 \cdot 10^{-03}$
$6.0 \cdot 10^{-01}$	$5.2310 \cdot 10^{-03}$	$1.3004 \cdot 10^{-01}$	$6.9967 \cdot 10^{-03}$	$1.3345 \cdot 10^{-04}$
$7.0 \cdot 10^{-01}$	$1.0313 \cdot 10^{-03}$	$7.3297 \cdot 10^{-02}$	$1.1537 \cdot 10^{-03}$	$1.1638 \cdot 10^{-05}$
$8.0 \cdot 10^{-01}$	$2.1805 \cdot 10^{-04}$	$3.2950 \cdot 10^{-02}$	$8.4013 \cdot 10^{-05}$	$8.8603 \cdot 10^{-07}$
$9.0 \cdot 10^{-01}$	$2.6290 \cdot 10^{-05}$	$8.4809 \cdot 10^{-03}$	$8.5046 \cdot 10^{-07}$	$2.8561 \cdot 10^{-08}$

Table 18: Same as table 13: VFNS, $\mu_F^2 = 10^2 \text{ GeV}^2$, $\mu_R^2/\mu_F^2 = 2$, $\alpha_s(\mu_F^2) = 0.1637695$.

x	$D_g^{\pi^+}(x, Q_0)$	$D_u^{\pi^+}(x, Q_0)$	$D_s^{\pi^+}(x, Q_0)$	$D_c^{\pi^+}(x, Q_0)$
$1.0 \cdot 10^{-02}$	$2.5055 \cdot 10^{+00}$	$1.9150 \cdot 10^{+00}$	$1.1192 \cdot 10^{+00}$	$1.5585 \cdot 10^{+00}$
$5.0 \cdot 10^{-02}$	$1.5215 \cdot 10^{+00}$	$1.5863 \cdot 10^{+00}$	$9.7389 \cdot 10^{-01}$	$7.6647 \cdot 10^{-01}$
$1.0 \cdot 10^{-01}$	$9.3252 \cdot 10^{-01}$	$1.1145 \cdot 10^{+00}$	$6.6353 \cdot 10^{-01}$	$3.6979 \cdot 10^{-01}$
$2.0 \cdot 10^{-01}$	$3.9236 \cdot 10^{-01}$	$6.2284 \cdot 10^{-01}$	$3.2456 \cdot 10^{-01}$	$1.0074 \cdot 10^{-01}$
$3.0 \cdot 10^{-01}$	$1.4328 \cdot 10^{-01}$	$3.7950 \cdot 10^{-01}$	$1.4449 \cdot 10^{-01}$	$2.5391 \cdot 10^{-02}$
$4.0 \cdot 10^{-01}$	$4.2628 \cdot 10^{-02}$	$2.4134 \cdot 10^{-01}$	$5.5238 \cdot 10^{-02}$	$5.2514 \cdot 10^{-03}$
$5.0 \cdot 10^{-01}$	$1.0403 \cdot 10^{-02}$	$1.5220 \cdot 10^{-01}$	$1.7218 \cdot 10^{-02}$	$8.1976 \cdot 10^{-04}$
$6.0 \cdot 10^{-01}$	$2.2992 \cdot 10^{-03}$	$8.9983 \cdot 10^{-02}$	$4.0074 \cdot 10^{-03}$	$8.9814 \cdot 10^{-05}$
$7.0 \cdot 10^{-01}$	$5.4993 \cdot 10^{-04}$	$4.6600 \cdot 10^{-02}$	$5.8831 \cdot 10^{-04}$	$7.3959 \cdot 10^{-06}$
$8.0 \cdot 10^{-01}$	$1.2453 \cdot 10^{-04}$	$1.8685 \cdot 10^{-02}$	$3.7254 \cdot 10^{-05}$	$6.0313 \cdot 10^{-07}$
$9.0 \cdot 10^{-01}$	$1.2788 \cdot 10^{-05}$	$3.9843 \cdot 10^{-03}$	$2.9477 \cdot 10^{-07}$	$1.4005 \cdot 10^{-08}$

Table 19: Same as table 13: VFNS, $\mu_F^2 = 10^3 \text{ GeV}^2$, $\mu_R^2/\mu_F^2 = 1/2$, $\alpha_s(\mu_F^2) = 0.1501564$.

x	$D_g^{\pi^+}(x, Q_0)$	$D_u^{\pi^+}(x, Q_0)$	$D_s^{\pi^+}(x, Q_0)$	$D_c^{\pi^+}(x, Q_0)$
$1.0 \cdot 10^{-02}$	$2.3873 \cdot 10^{+00}$	$1.9405 \cdot 10^{+00}$	$1.1453 \cdot 10^{+00}$	$1.4044 \cdot 10^{+00}$
$5.0 \cdot 10^{-02}$	$1.3242 \cdot 10^{+00}$	$1.4453 \cdot 10^{+00}$	$8.2905 \cdot 10^{-01}$	$6.4117 \cdot 10^{-01}$
$1.0 \cdot 10^{-01}$	$8.3590 \cdot 10^{-01}$	$1.0361 \cdot 10^{+00}$	$5.8054 \cdot 10^{-01}$	$3.1442 \cdot 10^{-01}$
$2.0 \cdot 10^{-01}$	$3.7371 \cdot 10^{-01}$	$6.0550 \cdot 10^{-01}$	$3.0363 \cdot 10^{-01}$	$8.9037 \cdot 10^{-02}$
$3.0 \cdot 10^{-01}$	$1.4356 \cdot 10^{-01}$	$3.8162 \cdot 10^{-01}$	$1.4253 \cdot 10^{-01}$	$2.3359 \cdot 10^{-02}$
$4.0 \cdot 10^{-01}$	$4.4636 \cdot 10^{-02}$	$2.4804 \cdot 10^{-01}$	$5.6760 \cdot 10^{-02}$	$5.0552 \cdot 10^{-03}$
$5.0 \cdot 10^{-01}$	$1.1303 \cdot 10^{-02}$	$1.5874 \cdot 10^{-01}$	$1.8272 \cdot 10^{-02}$	$8.3751 \cdot 10^{-04}$
$6.0 \cdot 10^{-01}$	$2.5472 \cdot 10^{-03}$	$9.5071 \cdot 10^{-02}$	$4.3682 \cdot 10^{-03}$	$1.0082 \cdot 10^{-04}$
$7.0 \cdot 10^{-01}$	$6.0528 \cdot 10^{-04}$	$4.9972 \cdot 10^{-02}$	$6.5773 \cdot 10^{-04}$	$9.5737 \cdot 10^{-06}$
$8.0 \cdot 10^{-01}$	$1.3583 \cdot 10^{-04}$	$2.0445 \cdot 10^{-02}$	$4.2971 \cdot 10^{-05}$	$8.4913 \cdot 10^{-07}$
$9.0 \cdot 10^{-01}$	$1.4014 \cdot 10^{-05}$	$4.5074 \cdot 10^{-03}$	$3.7152 \cdot 10^{-07}$	$2.5215 \cdot 10^{-08}$

Table 20: Same as table 13: VFNS, $\mu_F^2 = 10^3 \text{ GeV}^2$, $\mu_R^2/\mu_F^2 = 1$, $\alpha_s(\mu_F^2) = 0.1404546$.

x	$D_g^{\pi^+}(x, Q_0)$	$D_u^{\pi^+}(x, Q_0)$	$D_s^{\pi^+}(x, Q_0)$	$D_c^{\pi^+}(x, Q_0)$
$1.0 \cdot 10^{-02}$	$2.2233 \cdot 10^{+00}$	$1.8842 \cdot 10^{+00}$	$1.0876 \cdot 10^{+00}$	$1.2672 \cdot 10^{+00}$
$5.0 \cdot 10^{-02}$	$1.2150 \cdot 10^{+00}$	$1.3672 \cdot 10^{+00}$	$7.4390 \cdot 10^{-01}$	$5.6957 \cdot 10^{-01}$
$1.0 \cdot 10^{-01}$	$7.9516 \cdot 10^{-01}$	$1.0004 \cdot 10^{+00}$	$5.3729 \cdot 10^{-01}$	$2.8555 \cdot 10^{-01}$
$2.0 \cdot 10^{-01}$	$3.7904 \cdot 10^{-01}$	$6.0485 \cdot 10^{-01}$	$2.9735 \cdot 10^{-01}$	$8.4231 \cdot 10^{-02}$
$3.0 \cdot 10^{-01}$	$1.5315 \cdot 10^{-01}$	$3.9051 \cdot 10^{-01}$	$1.4548 \cdot 10^{-01}$	$2.2956 \cdot 10^{-02}$
$4.0 \cdot 10^{-01}$	$4.9562 \cdot 10^{-02}$	$2.5810 \cdot 10^{-01}$	$5.9804 \cdot 10^{-02}$	$5.1639 \cdot 10^{-03}$
$5.0 \cdot 10^{-01}$	$1.2888 \cdot 10^{-02}$	$1.6741 \cdot 10^{-01}$	$1.9758 \cdot 10^{-02}$	$8.9297 \cdot 10^{-04}$
$6.0 \cdot 10^{-01}$	$2.9074 \cdot 10^{-03}$	$1.0162 \cdot 10^{-01}$	$4.8342 \cdot 10^{-03}$	$1.1312 \cdot 10^{-04}$
$7.0 \cdot 10^{-01}$	$6.7562 \cdot 10^{-04}$	$5.4272 \cdot 10^{-02}$	$7.4501 \cdot 10^{-04}$	$1.1337 \cdot 10^{-05}$
$8.0 \cdot 10^{-01}$	$1.5053 \cdot 10^{-04}$	$2.2688 \cdot 10^{-02}$	$5.0079 \cdot 10^{-05}$	$1.0444 \cdot 10^{-06}$
$9.0 \cdot 10^{-01}$	$1.5798 \cdot 10^{-05}$	$5.1832 \cdot 10^{-03}$	$4.6023 \cdot 10^{-07}$	$3.5222 \cdot 10^{-08}$

Table 21: Same as table 13: VFNS, $\mu_F^2 = 10^3 \text{ GeV}^2$, $\mu_R^2/\mu_F^2 = 2$, $\alpha_s(\mu_F^2) = 0.1316906$.

x	$D_g^{\pi^+}(x, Q_0)$	$D_u^{\pi^+}(x, Q_0)$	$D_s^{\pi^+}(x, Q_0)$	$D_c^{\pi^+}(x, Q_0)$
$1.0 \cdot 10^{-02}$	$3.2870 \cdot 10^{+00}$	$2.3905 \cdot 10^{+00}$	$1.6064 \cdot 10^{+00}$	$1.9877 \cdot 10^{+00}$
$5.0 \cdot 10^{-02}$	$1.5277 \cdot 10^{+00}$	$1.6309 \cdot 10^{+00}$	$1.0465 \cdot 10^{+00}$	$8.2966 \cdot 10^{-01}$
$1.0 \cdot 10^{-01}$	$8.3390 \cdot 10^{-01}$	$1.0812 \cdot 10^{+00}$	$6.5709 \cdot 10^{-01}$	$3.7534 \cdot 10^{-01}$
$2.0 \cdot 10^{-01}$	$2.9811 \cdot 10^{-01}$	$5.7123 \cdot 10^{-01}$	$2.9337 \cdot 10^{-01}$	$9.4061 \cdot 10^{-02}$
$3.0 \cdot 10^{-01}$	$9.6880 \cdot 10^{-02}$	$3.3697 \cdot 10^{-01}$	$1.2270 \cdot 10^{-01}$	$2.2257 \cdot 10^{-02}$
$4.0 \cdot 10^{-01}$	$2.6760 \cdot 10^{-02}$	$2.0844 \cdot 10^{-01}$	$4.4550 \cdot 10^{-02}$	$4.3784 \cdot 10^{-03}$
$5.0 \cdot 10^{-01}$	$6.4771 \cdot 10^{-03}$	$1.2750 \cdot 10^{-01}$	$1.3238 \cdot 10^{-02}$	$6.6282 \cdot 10^{-04}$
$6.0 \cdot 10^{-01}$	$1.5557 \cdot 10^{-03}$	$7.2690 \cdot 10^{-02}$	$2.9347 \cdot 10^{-03}$	$7.4275 \cdot 10^{-05}$
$7.0 \cdot 10^{-01}$	$4.0416 \cdot 10^{-04}$	$3.5993 \cdot 10^{-02}$	$4.0828 \cdot 10^{-04}$	$7.0423 \cdot 10^{-06}$
$8.0 \cdot 10^{-01}$	$8.8370 \cdot 10^{-05}$	$1.3588 \cdot 10^{-02}$	$2.4246 \cdot 10^{-05}$	$6.4291 \cdot 10^{-07}$
$9.0 \cdot 10^{-01}$	$7.9382 \cdot 10^{-06}$	$2.6253 \cdot 10^{-03}$	$1.7799 \cdot 10^{-07}$	$1.6186 \cdot 10^{-08}$

Table 22: Same as table 13: VFNS, $\mu_F^2 = 10^4 \text{ GeV}^2$, $\mu_R^2/\mu_F^2 = 1/2$, $\alpha_s(\mu_F^2) = 0.1228358$.

x	$D_g^{\pi^+}(x, Q_0)$	$D_u^{\pi^+}(x, Q_0)$	$D_s^{\pi^+}(x, Q_0)$	$D_c^{\pi^+}(x, Q_0)$
$1.0 \cdot 10^{-02}$	$3.0177 \cdot 10^{+00}$	$2.3322 \cdot 10^{+00}$	$1.5485 \cdot 10^{+00}$	$1.7693 \cdot 10^{+00}$
$5.0 \cdot 10^{-02}$	$1.3404 \cdot 10^{+00}$	$1.4855 \cdot 10^{+00}$	$8.9706 \cdot 10^{-01}$	$7.0101 \cdot 10^{-01}$
$1.0 \cdot 10^{-01}$	$7.5535 \cdot 10^{-01}$	$1.0082 \cdot 10^{+00}$	$5.7953 \cdot 10^{-01}$	$3.2288 \cdot 10^{-01}$
$2.0 \cdot 10^{-01}$	$2.8672 \cdot 10^{-01}$	$5.5778 \cdot 10^{-01}$	$2.7622 \cdot 10^{-01}$	$8.4158 \cdot 10^{-02}$
$3.0 \cdot 10^{-01}$	$9.7934 \cdot 10^{-02}$	$3.4018 \cdot 10^{-01}$	$1.2168 \cdot 10^{-01}$	$2.0730 \cdot 10^{-02}$
$4.0 \cdot 10^{-01}$	$2.8222 \cdot 10^{-02}$	$2.1494 \cdot 10^{-01}$	$4.5993 \cdot 10^{-02}$	$4.2677 \cdot 10^{-03}$
$5.0 \cdot 10^{-01}$	$7.0525 \cdot 10^{-03}$	$1.3341 \cdot 10^{-01}$	$1.4109 \cdot 10^{-02}$	$6.8549 \cdot 10^{-04}$
$6.0 \cdot 10^{-01}$	$1.7140 \cdot 10^{-03}$	$7.7074 \cdot 10^{-02}$	$3.2124 \cdot 10^{-03}$	$8.3824 \cdot 10^{-05}$
$7.0 \cdot 10^{-01}$	$4.4339 \cdot 10^{-04}$	$3.8755 \cdot 10^{-02}$	$4.5846 \cdot 10^{-04}$	$8.8037 \cdot 10^{-06}$
$8.0 \cdot 10^{-01}$	$9.7044 \cdot 10^{-05}$	$1.4938 \cdot 10^{-02}$	$2.8103 \cdot 10^{-05}$	$8.3715 \cdot 10^{-07}$
$9.0 \cdot 10^{-01}$	$8.8491 \cdot 10^{-06}$	$2.9872 \cdot 10^{-03}$	$2.2567 \cdot 10^{-07}$	$2.4436 \cdot 10^{-08}$

Table 23: Same as table 13: VFNS, $\mu_F^2 = 10^4 \text{ GeV}^2$, $\mu_R^2/\mu_F^2 = 1$, $\alpha_s(\mu_F^2) = 0.1163266$.

x	$D_g^{\pi^+}(x, Q_0)$	$D_u^{\pi^+}(x, Q_0)$	$D_s^{\pi^+}(x, Q_0)$	$D_c^{\pi^+}(x, Q_0)$
$1.0 \cdot 10^{-02}$	$2.7851 \cdot 10^{+00}$	$2.2317 \cdot 10^{+00}$	$1.4460 \cdot 10^{+00}$	$1.5968 \cdot 10^{+00}$
$5.0 \cdot 10^{-02}$	$1.2438 \cdot 10^{+00}$	$1.4079 \cdot 10^{+00}$	$8.1203 \cdot 10^{-01}$	$6.2973 \cdot 10^{-01}$
$1.0 \cdot 10^{-01}$	$7.2742 \cdot 10^{-01}$	$9.7721 \cdot 10^{-01}$	$5.4096 \cdot 10^{-01}$	$2.9692 \cdot 10^{-01}$
$2.0 \cdot 10^{-01}$	$2.9399 \cdot 10^{-01}$	$5.5973 \cdot 10^{-01}$	$2.7236 \cdot 10^{-01}$	$8.0665 \cdot 10^{-02}$
$3.0 \cdot 10^{-01}$	$1.0543 \cdot 10^{-01}$	$3.4959 \cdot 10^{-01}$	$1.2494 \cdot 10^{-01}$	$2.0642 \cdot 10^{-02}$
$4.0 \cdot 10^{-01}$	$3.1514 \cdot 10^{-02}$	$2.2459 \cdot 10^{-01}$	$4.8735 \cdot 10^{-02}$	$4.4159 \cdot 10^{-03}$
$5.0 \cdot 10^{-01}$	$8.0281 \cdot 10^{-03}$	$1.4131 \cdot 10^{-01}$	$1.5344 \cdot 10^{-02}$	$7.3941 \cdot 10^{-04}$
$6.0 \cdot 10^{-01}$	$1.9391 \cdot 10^{-03}$	$8.2795 \cdot 10^{-02}$	$3.5763 \cdot 10^{-03}$	$9.4646 \cdot 10^{-05}$
$7.0 \cdot 10^{-01}$	$4.9426 \cdot 10^{-04}$	$4.2336 \cdot 10^{-02}$	$5.2269 \cdot 10^{-04}$	$1.0331 \cdot 10^{-05}$
$8.0 \cdot 10^{-01}$	$1.0864 \cdot 10^{-04}$	$1.6691 \cdot 10^{-02}$	$3.2993 \cdot 10^{-05}$	$1.0083 \cdot 10^{-06}$
$9.0 \cdot 10^{-01}$	$1.0149 \cdot 10^{-05}$	$3.4642 \cdot 10^{-03}$	$2.8196 \cdot 10^{-07}$	$3.2481 \cdot 10^{-08}$

Table 24: Same as table 13: VFNS, $\mu_F^2 = 10^4 \text{ GeV}^2$, $\mu_R^2/\mu_F^2 = 2$, $\alpha_s(\mu_F^2) = 0.1102998$.

x	$D_g^{\pi^+}(x, Q_0)$	$D_u^{\pi^+}(x, Q_0)$	$D_s^{\pi^+}(x, Q_0)$
$1.0 \cdot 10^{-02}$	$-1.8792 \cdot 10^{+00}$	$-4.7902 \cdot 10^{-01}$	$-1.3037 \cdot 10^{+00}$
$5.0 \cdot 10^{-02}$	$6.9280 \cdot 10^{-01}$	$1.0172 \cdot 10^{+00}$	$3.1863 \cdot 10^{-01}$
$1.0 \cdot 10^{-01}$	$9.1279 \cdot 10^{-01}$	$1.0561 \cdot 10^{+00}$	$5.1619 \cdot 10^{-01}$
$2.0 \cdot 10^{-01}$	$7.5327 \cdot 10^{-01}$	$7.7432 \cdot 10^{-01}$	$4.1056 \cdot 10^{-01}$
$3.0 \cdot 10^{-01}$	$4.2646 \cdot 10^{-01}$	$5.3095 \cdot 10^{-01}$	$2.3102 \cdot 10^{-01}$
$4.0 \cdot 10^{-01}$	$1.7559 \cdot 10^{-01}$	$3.6539 \cdot 10^{-01}$	$1.0401 \cdot 10^{-01}$
$5.0 \cdot 10^{-01}$	$5.2453 \cdot 10^{-02}$	$2.5022 \cdot 10^{-01}$	$3.7271 \cdot 10^{-02}$
$6.0 \cdot 10^{-01}$	$1.1152 \cdot 10^{-02}$	$1.6363 \cdot 10^{-01}$	$9.9634 \cdot 10^{-03}$
$7.0 \cdot 10^{-01}$	$1.8531 \cdot 10^{-03}$	$9.6265 \cdot 10^{-02}$	$1.7089 \cdot 10^{-03}$
$8.0 \cdot 10^{-01}$	$3.5067 \cdot 10^{-04}$	$4.5884 \cdot 10^{-02}$	$1.3207 \cdot 10^{-04}$
$9.0 \cdot 10^{-01}$	$5.2702 \cdot 10^{-05}$	$1.2993 \cdot 10^{-02}$	$1.5603 \cdot 10^{-06}$

Table 25: Numerical values of gluon, up and strange FFs evolved at NNLO in the FFNS up to $\mu_F^2 = 10 \text{ GeV}^2$, $\mu_R^2/\mu_F^2 = 1/2$, $\alpha_s(\mu_F^2) = 0.2749250$.

x	$D_g^{\pi^+}(x, Q_0)$	$D_u^{\pi^+}(x, Q_0)$	$D_s^{\pi^+}(x, Q_0)$
$1.0 \cdot 10^{-02}$	$-5.2241 \cdot 10^{-01}$	$3.5771 \cdot 10^{-01}$	$-4.6473 \cdot 10^{-01}$
$5.0 \cdot 10^{-02}$	$8.0768 \cdot 10^{-01}$	$1.1145 \cdot 10^{+00}$	$4.1771 \cdot 10^{-01}$
$1.0 \cdot 10^{-01}$	$8.7624 \cdot 10^{-01}$	$1.0316 \cdot 10^{+00}$	$4.9234 \cdot 10^{-01}$
$2.0 \cdot 10^{-01}$	$7.1263 \cdot 10^{-01}$	$7.4120 \cdot 10^{-01}$	$3.7806 \cdot 10^{-01}$
$3.0 \cdot 10^{-01}$	$4.1162 \cdot 10^{-01}$	$5.1782 \cdot 10^{-01}$	$2.1820 \cdot 10^{-01}$
$4.0 \cdot 10^{-01}$	$1.7300 \cdot 10^{-01}$	$3.6346 \cdot 10^{-01}$	$1.0125 \cdot 10^{-01}$
$5.0 \cdot 10^{-01}$	$5.2577 \cdot 10^{-02}$	$2.5221 \cdot 10^{-01}$	$3.7282 \cdot 10^{-02}$
$6.0 \cdot 10^{-01}$	$1.1250 \cdot 10^{-02}$	$1.6637 \cdot 10^{-01}$	$1.0191 \cdot 10^{-02}$
$7.0 \cdot 10^{-01}$	$1.8117 \cdot 10^{-03}$	$9.8662 \cdot 10^{-02}$	$1.7793 \cdot 10^{-03}$
$8.0 \cdot 10^{-01}$	$3.2016 \cdot 10^{-04}$	$4.7515 \cdot 10^{-02}$	$1.3923 \cdot 10^{-04}$
$9.0 \cdot 10^{-01}$	$4.6958 \cdot 10^{-05}$	$1.3691 \cdot 10^{-02}$	$1.5652 \cdot 10^{-06}$

Table 26: Same as table 25: FFNS, $\mu_F^2 = 10 \text{ GeV}^2$, $\mu_R^2/\mu_F^2 = 1$, $\alpha_s(\mu_F^2) = 0.2369645$.

x	$D_g^{\pi^+}(x, Q_0)$	$D_u^{\pi^+}(x, Q_0)$	$D_s^{\pi^+}(x, Q_0)$
$1.0 \cdot 10^{-02}$	$-2.1326 \cdot 10^{-02}$	$6.7241 \cdot 10^{-01}$	$-1.4945 \cdot 10^{-01}$
$5.0 \cdot 10^{-02}$	$7.9209 \cdot 10^{-01}$	$1.1159 \cdot 10^{+00}$	$4.1707 \cdot 10^{-01}$
$1.0 \cdot 10^{-01}$	$8.2704 \cdot 10^{-01}$	$1.0026 \cdot 10^{+00}$	$4.6041 \cdot 10^{-01}$
$2.0 \cdot 10^{-01}$	$6.9265 \cdot 10^{-01}$	$7.2545 \cdot 10^{-01}$	$3.6024 \cdot 10^{-01}$
$3.0 \cdot 10^{-01}$	$4.1308 \cdot 10^{-01}$	$5.1581 \cdot 10^{-01}$	$2.1411 \cdot 10^{-01}$
$4.0 \cdot 10^{-01}$	$1.7841 \cdot 10^{-01}$	$3.6738 \cdot 10^{-01}$	$1.0192 \cdot 10^{-01}$
$5.0 \cdot 10^{-01}$	$5.5504 \cdot 10^{-02}$	$2.5756 \cdot 10^{-01}$	$3.8335 \cdot 10^{-02}$
$6.0 \cdot 10^{-01}$	$1.2063 \cdot 10^{-02}$	$1.7131 \cdot 10^{-01}$	$1.0668 \cdot 10^{-02}$
$7.0 \cdot 10^{-01}$	$1.9185 \cdot 10^{-03}$	$1.0250 \cdot 10^{-01}$	$1.8924 \cdot 10^{-03}$
$8.0 \cdot 10^{-01}$	$3.2144 \cdot 10^{-04}$	$4.9950 \cdot 10^{-02}$	$1.5055 \cdot 10^{-04}$
$9.0 \cdot 10^{-01}$	$4.5968 \cdot 10^{-05}$	$1.4680 \cdot 10^{-02}$	$1.7142 \cdot 10^{-06}$

Table 27: Same as table 25: FFNS, $\mu_F^2 = 10 \text{ GeV}^2$, $\mu_R^2/\mu_F^2 = 2$, $\alpha_s(\mu_F^2) = 0.2087674$.

x	$D_g^{\pi^+}(x, Q_0)$	$D_u^{\pi^+}(x, Q_0)$	$D_s^{\pi^+}(x, Q_0)$
$1.0 \cdot 10^{-02}$	$-9.2616 \cdot 10^{-01}$	$-2.4841 \cdot 10^{-01}$	$-1.0610 \cdot 10^{+00}$
$5.0 \cdot 10^{-02}$	$1.2010 \cdot 10^{+00}$	$1.2584 \cdot 10^{+00}$	$6.0423 \cdot 10^{-01}$
$1.0 \cdot 10^{-01}$	$1.0385 \cdot 10^{+00}$	$1.1216 \cdot 10^{+00}$	$6.2957 \cdot 10^{-01}$
$2.0 \cdot 10^{-01}$	$5.8416 \cdot 10^{-01}$	$7.1622 \cdot 10^{-01}$	$3.8735 \cdot 10^{-01}$
$3.0 \cdot 10^{-01}$	$2.5511 \cdot 10^{-01}$	$4.5378 \cdot 10^{-01}$	$1.8854 \cdot 10^{-01}$
$4.0 \cdot 10^{-01}$	$8.6015 \cdot 10^{-02}$	$2.9513 \cdot 10^{-01}$	$7.6046 \cdot 10^{-02}$
$5.0 \cdot 10^{-01}$	$2.2294 \cdot 10^{-02}$	$1.9170 \cdot 10^{-01}$	$2.4786 \cdot 10^{-02}$
$6.0 \cdot 10^{-01}$	$4.6376 \cdot 10^{-03}$	$1.1809 \cdot 10^{-01}$	$6.0531 \cdot 10^{-03}$
$7.0 \cdot 10^{-01}$	$9.4689 \cdot 10^{-04}$	$6.4518 \cdot 10^{-02}$	$9.4394 \cdot 10^{-04}$
$8.0 \cdot 10^{-01}$	$2.0893 \cdot 10^{-04}$	$2.7820 \cdot 10^{-02}$	$6.5371 \cdot 10^{-05}$
$9.0 \cdot 10^{-01}$	$2.4937 \cdot 10^{-05}$	$6.6798 \cdot 10^{-03}$	$6.9517 \cdot 10^{-07}$

Table 28: Same as table 25: FFNS, $\mu_F^2 = 10^2 \text{ GeV}^2$, $\mu_R^2/\mu_F^2 = 1/2$, $\alpha_s(\mu_F^2) = 0.1808461$.

x	$D_g^{\pi^+}(x, Q_0)$	$D_u^{\pi^+}(x, Q_0)$	$D_s^{\pi^+}(x, Q_0)$
$1.0 \cdot 10^{-02}$	$4.3018 \cdot 10^{-01}$	$7.0077 \cdot 10^{-01}$	$-1.0938 \cdot 10^{-01}$
$5.0 \cdot 10^{-02}$	$1.2356 \cdot 10^{+00}$	$1.3198 \cdot 10^{+00}$	$6.6718 \cdot 10^{-01}$
$1.0 \cdot 10^{-01}$	$9.8493 \cdot 10^{-01}$	$1.0845 \cdot 10^{+00}$	$5.9300 \cdot 10^{-01}$
$2.0 \cdot 10^{-01}$	$5.5526 \cdot 10^{-01}$	$6.8698 \cdot 10^{-01}$	$3.5853 \cdot 10^{-01}$
$3.0 \cdot 10^{-01}$	$2.4764 \cdot 10^{-01}$	$4.4447 \cdot 10^{-01}$	$1.7907 \cdot 10^{-01}$
$4.0 \cdot 10^{-01}$	$8.5205 \cdot 10^{-02}$	$2.9474 \cdot 10^{-01}$	$7.4407 \cdot 10^{-02}$
$5.0 \cdot 10^{-01}$	$2.2425 \cdot 10^{-02}$	$1.9390 \cdot 10^{-01}$	$2.4911 \cdot 10^{-02}$
$6.0 \cdot 10^{-01}$	$4.6706 \cdot 10^{-03}$	$1.2050 \cdot 10^{-01}$	$6.2193 \cdot 10^{-03}$
$7.0 \cdot 10^{-01}$	$9.3228 \cdot 10^{-04}$	$6.6410 \cdot 10^{-02}$	$9.8675 \cdot 10^{-04}$
$8.0 \cdot 10^{-01}$	$2.0213 \cdot 10^{-04}$	$2.8963 \cdot 10^{-02}$	$6.9032 \cdot 10^{-05}$
$9.0 \cdot 10^{-01}$	$2.4256 \cdot 10^{-05}$	$7.0874 \cdot 10^{-03}$	$6.8263 \cdot 10^{-07}$

Table 29: Same as table 25: FFNS, $\mu_F^2 = 10^2 \text{ GeV}^2$, $\mu_R^2/\mu_F^2 = 1$, $\alpha_s(\mu_F^2) = 0.1644438$.

x	$D_g^{\pi^+}(x, Q_0)$	$D_u^{\pi^+}(x, Q_0)$	$D_s^{\pi^+}(x, Q_0)$
$1.0 \cdot 10^{-02}$	$8.7835 \cdot 10^{-01}$	$1.0344 \cdot 10^{+00}$	$2.2467 \cdot 10^{-01}$
$5.0 \cdot 10^{-02}$	$1.1872 \cdot 10^{+00}$	$1.3021 \cdot 10^{+00}$	$6.4691 \cdot 10^{-01}$
$1.0 \cdot 10^{-01}$	$9.3764 \cdot 10^{-01}$	$1.0515 \cdot 10^{+00}$	$5.5676 \cdot 10^{-01}$
$2.0 \cdot 10^{-01}$	$5.4582 \cdot 10^{-01}$	$6.7498 \cdot 10^{-01}$	$3.4415 \cdot 10^{-01}$
$3.0 \cdot 10^{-01}$	$2.5133 \cdot 10^{-01}$	$4.4508 \cdot 10^{-01}$	$1.7702 \cdot 10^{-01}$
$4.0 \cdot 10^{-01}$	$8.8871 \cdot 10^{-02}$	$2.9953 \cdot 10^{-01}$	$7.5476 \cdot 10^{-02}$
$5.0 \cdot 10^{-01}$	$2.3895 \cdot 10^{-02}$	$1.9914 \cdot 10^{-01}$	$2.5824 \cdot 10^{-02}$
$6.0 \cdot 10^{-01}$	$5.0127 \cdot 10^{-03}$	$1.2489 \cdot 10^{-01}$	$6.5675 \cdot 10^{-03}$
$7.0 \cdot 10^{-01}$	$9.8118 \cdot 10^{-04}$	$6.9528 \cdot 10^{-02}$	$1.0596 \cdot 10^{-03}$
$8.0 \cdot 10^{-01}$	$2.0853 \cdot 10^{-04}$	$3.0739 \cdot 10^{-02}$	$7.5407 \cdot 10^{-05}$
$9.0 \cdot 10^{-01}$	$2.5117 \cdot 10^{-05}$	$7.6942 \cdot 10^{-03}$	$7.4918 \cdot 10^{-07}$

Table 30: Same as table 25: FFNS, $\mu_F^2 = 10^2 \text{ GeV}^2$, $\mu_R^2/\mu_F^2 = 2$, $\alpha_s(\mu_F^2) = 0.1508899$.

x	$D_g^{\pi^+}(x, Q_0)$	$D_u^{\pi^+}(x, Q_0)$	$D_s^{\pi^+}(x, Q_0)$
$1.0 \cdot 10^{-02}$	$1.6184 \cdot 10^{-01}$	$1.8297 \cdot 10^{-01}$	$-6.1839 \cdot 10^{-01}$
$5.0 \cdot 10^{-02}$	$1.4257 \cdot 10^{+00}$	$1.3940 \cdot 10^{+00}$	$7.7217 \cdot 10^{-01}$
$1.0 \cdot 10^{-01}$	$1.0082 \cdot 10^{+00}$	$1.1231 \cdot 10^{+00}$	$6.6379 \cdot 10^{-01}$
$2.0 \cdot 10^{-01}$	$4.5375 \cdot 10^{-01}$	$6.5868 \cdot 10^{-01}$	$3.5427 \cdot 10^{-01}$
$3.0 \cdot 10^{-01}$	$1.6934 \cdot 10^{-01}$	$3.9875 \cdot 10^{-01}$	$1.5840 \cdot 10^{-01}$
$4.0 \cdot 10^{-01}$	$5.0877 \cdot 10^{-02}$	$2.5062 \cdot 10^{-01}$	$5.9787 \cdot 10^{-02}$
$5.0 \cdot 10^{-01}$	$1.2428 \cdot 10^{-02}$	$1.5713 \cdot 10^{-01}$	$1.8366 \cdot 10^{-02}$
$6.0 \cdot 10^{-01}$	$2.7101 \cdot 10^{-03}$	$9.2822 \cdot 10^{-02}$	$4.2298 \cdot 10^{-03}$
$7.0 \cdot 10^{-01}$	$6.3006 \cdot 10^{-04}$	$4.8139 \cdot 10^{-02}$	$6.1899 \cdot 10^{-04}$
$8.0 \cdot 10^{-01}$	$1.3909 \cdot 10^{-04}$	$1.9346 \cdot 10^{-02}$	$3.9802 \cdot 10^{-05}$
$9.0 \cdot 10^{-01}$	$1.4025 \cdot 10^{-05}$	$4.1386 \cdot 10^{-03}$	$3.9353 \cdot 10^{-07}$

Table 31: Same as table 25: FFNS, $\mu_F^2 = 10^3 \text{ GeV}^2$, $\mu_R^2/\mu_F^2 = 1/2$, $\alpha_s(\mu_F^2) = 0.1361858$.

x	$D_g^{\pi^+}(x, Q_0)$	$D_u^{\pi^+}(x, Q_0)$	$D_s^{\pi^+}(x, Q_0)$
$1.0 \cdot 10^{-02}$	$1.3748 \cdot 10^{+00}$	$1.1309 \cdot 10^{+00}$	$3.3200 \cdot 10^{-01}$
$5.0 \cdot 10^{-02}$	$1.4172 \cdot 10^{+00}$	$1.4306 \cdot 10^{+00}$	$8.1015 \cdot 10^{-01}$
$1.0 \cdot 10^{-01}$	$9.5459 \cdot 10^{-01}$	$1.0821 \cdot 10^{+00}$	$6.2332 \cdot 10^{-01}$
$2.0 \cdot 10^{-01}$	$4.3327 \cdot 10^{-01}$	$6.3347 \cdot 10^{-01}$	$3.2929 \cdot 10^{-01}$
$3.0 \cdot 10^{-01}$	$1.6513 \cdot 10^{-01}$	$3.9183 \cdot 10^{-01}$	$1.5105 \cdot 10^{-01}$
$4.0 \cdot 10^{-01}$	$5.0591 \cdot 10^{-02}$	$2.5091 \cdot 10^{-01}$	$5.8690 \cdot 10^{-02}$
$5.0 \cdot 10^{-01}$	$1.2527 \cdot 10^{-02}$	$1.5924 \cdot 10^{-01}$	$1.8506 \cdot 10^{-02}$
$6.0 \cdot 10^{-01}$	$2.7322 \cdot 10^{-03}$	$9.4895 \cdot 10^{-02}$	$4.3543 \cdot 10^{-03}$
$7.0 \cdot 10^{-01}$	$6.2833 \cdot 10^{-04}$	$4.9650 \cdot 10^{-02}$	$6.4788 \cdot 10^{-04}$
$8.0 \cdot 10^{-01}$	$1.3864 \cdot 10^{-04}$	$2.0188 \cdot 10^{-02}$	$4.2019 \cdot 10^{-05}$
$9.0 \cdot 10^{-01}$	$1.4184 \cdot 10^{-05}$	$4.4034 \cdot 10^{-03}$	$3.8275 \cdot 10^{-07}$

Table 32: Same as table 25: FFNS, $\mu_F^2 = 10^3 \text{ GeV}^2$, $\mu_R^2/\mu_F^2 = 1$, $\alpha_s(\mu_F^2) = 0.1269012$.

x	$D_g^{\pi^+}(x, Q_0)$	$D_u^{\pi^+}(x, Q_0)$	$D_s^{\pi^+}(x, Q_0)$
$1.0 \cdot 10^{-02}$	$1.7277 \cdot 10^{+00}$	$1.4412 \cdot 10^{+00}$	$6.4263 \cdot 10^{-01}$
$5.0 \cdot 10^{-02}$	$1.3585 \cdot 10^{+00}$	$1.4033 \cdot 10^{+00}$	$7.8017 \cdot 10^{-01}$
$1.0 \cdot 10^{-01}$	$9.1554 \cdot 10^{-01}$	$1.0502 \cdot 10^{+00}$	$5.8810 \cdot 10^{-01}$
$2.0 \cdot 10^{-01}$	$4.2926 \cdot 10^{-01}$	$6.2449 \cdot 10^{-01}$	$3.1782 \cdot 10^{-01}$
$3.0 \cdot 10^{-01}$	$1.6872 \cdot 10^{-01}$	$3.9367 \cdot 10^{-01}$	$1.5000 \cdot 10^{-01}$
$4.0 \cdot 10^{-01}$	$5.3029 \cdot 10^{-02}$	$2.5572 \cdot 10^{-01}$	$5.9770 \cdot 10^{-02}$
$5.0 \cdot 10^{-01}$	$1.3363 \cdot 10^{-02}$	$1.6399 \cdot 10^{-01}$	$1.9252 \cdot 10^{-02}$
$6.0 \cdot 10^{-01}$	$2.9173 \cdot 10^{-03}$	$9.8636 \cdot 10^{-02}$	$4.6135 \cdot 10^{-03}$
$7.0 \cdot 10^{-01}$	$6.6102 \cdot 10^{-04}$	$5.2156 \cdot 10^{-02}$	$6.9805 \cdot 10^{-04}$
$8.0 \cdot 10^{-01}$	$1.4527 \cdot 10^{-04}$	$2.1510 \cdot 10^{-02}$	$4.6040 \cdot 10^{-05}$
$9.0 \cdot 10^{-01}$	$1.5065 \cdot 10^{-05}$	$4.8033 \cdot 10^{-03}$	$4.1953 \cdot 10^{-07}$

Table 33: Same as table 25: FFNS, $\mu_F^2 = 10^3 \text{ GeV}^2$, $\mu_R^2/\mu_F^2 = 2$, $\alpha_s(\mu_F^2) = 0.1188431$.

x	$D_g^{\pi^+}(x, Q_0)$	$D_u^{\pi^+}(x, Q_0)$	$D_s^{\pi^+}(x, Q_0)$
$1.0 \cdot 10^{-02}$	$1.0772 \cdot 10^{+00}$	$6.0595 \cdot 10^{-01}$	$-1.8519 \cdot 10^{-01}$
$5.0 \cdot 10^{-02}$	$1.5140 \cdot 10^{+00}$	$1.4696 \cdot 10^{+00}$	$8.7330 \cdot 10^{-01}$
$1.0 \cdot 10^{-01}$	$9.3978 \cdot 10^{-01}$	$1.1033 \cdot 10^{+00}$	$6.6882 \cdot 10^{-01}$
$2.0 \cdot 10^{-01}$	$3.6193 \cdot 10^{-01}$	$6.1004 \cdot 10^{-01}$	$3.2441 \cdot 10^{-01}$
$3.0 \cdot 10^{-01}$	$1.2108 \cdot 10^{-01}$	$3.5792 \cdot 10^{-01}$	$1.3670 \cdot 10^{-01}$
$4.0 \cdot 10^{-01}$	$3.3810 \cdot 10^{-02}$	$2.1940 \cdot 10^{-01}$	$4.9203 \cdot 10^{-02}$
$5.0 \cdot 10^{-01}$	$8.1014 \cdot 10^{-03}$	$1.3386 \cdot 10^{-01}$	$1.4472 \cdot 10^{-02}$
$6.0 \cdot 10^{-01}$	$1.8753 \cdot 10^{-03}$	$7.6532 \cdot 10^{-02}$	$3.1898 \cdot 10^{-03}$
$7.0 \cdot 10^{-01}$	$4.6737 \cdot 10^{-04}$	$3.8109 \cdot 10^{-02}$	$4.4482 \cdot 10^{-04}$
$8.0 \cdot 10^{-01}$	$9.9960 \cdot 10^{-05}$	$1.4500 \cdot 10^{-02}$	$2.7031 \cdot 10^{-05}$
$9.0 \cdot 10^{-01}$	$8.8903 \cdot 10^{-06}$	$2.8360 \cdot 10^{-03}$	$2.5268 \cdot 10^{-07}$

Table 34: Same as table 25: FFNS, $\mu_F^2 = 10^4 \text{ GeV}^2$, $\mu_R^2/\mu_F^2 = 1/2$, $\alpha_s(\mu_F^2) = 0.1096856$.

x	$D_g^{\pi^+}(x, Q_0)$	$D_u^{\pi^+}(x, Q_0)$	$D_s^{\pi^+}(x, Q_0)$
$1.0 \cdot 10^{-02}$	$2.1401 \cdot 10^{+00}$	$1.5232 \cdot 10^{+00}$	$7.3458 \cdot 10^{-01}$
$5.0 \cdot 10^{-02}$	$1.4826 \cdot 10^{+00}$	$1.4896 \cdot 10^{+00}$	$8.9453 \cdot 10^{-01}$
$1.0 \cdot 10^{-01}$	$8.9001 \cdot 10^{-01}$	$1.0615 \cdot 10^{+00}$	$6.2736 \cdot 10^{-01}$
$2.0 \cdot 10^{-01}$	$3.4683 \cdot 10^{-01}$	$5.8798 \cdot 10^{-01}$	$3.0245 \cdot 10^{-01}$
$3.0 \cdot 10^{-01}$	$1.1850 \cdot 10^{-01}$	$3.5255 \cdot 10^{-01}$	$1.3073 \cdot 10^{-01}$
$4.0 \cdot 10^{-01}$	$3.3718 \cdot 10^{-02}$	$2.2005 \cdot 10^{-01}$	$4.8411 \cdot 10^{-02}$
$5.0 \cdot 10^{-01}$	$8.1802 \cdot 10^{-03}$	$1.3584 \cdot 10^{-01}$	$1.4607 \cdot 10^{-02}$
$6.0 \cdot 10^{-01}$	$1.8956 \cdot 10^{-03}$	$7.8336 \cdot 10^{-02}$	$3.2876 \cdot 10^{-03}$
$7.0 \cdot 10^{-01}$	$4.7094 \cdot 10^{-04}$	$3.9357 \cdot 10^{-02}$	$4.6589 \cdot 10^{-04}$
$8.0 \cdot 10^{-01}$	$1.0137 \cdot 10^{-04}$	$1.5152 \cdot 10^{-02}$	$2.8525 \cdot 10^{-05}$
$9.0 \cdot 10^{-01}$	$9.1822 \cdot 10^{-06}$	$3.0223 \cdot 10^{-03}$	$2.4445 \cdot 10^{-07}$

Table 35: Same as table 25: FFNS, $\mu_F^2 = 10^4 \text{ GeV}^2$, $\mu_R^2/\mu_F^2 = 1$, $\alpha_s(\mu_F^2) = 0.1036710$.

x	$D_g^{\pi^+}(x, Q_0)$	$D_u^{\pi^+}(x, Q_0)$	$D_s^{\pi^+}(x, Q_0)$
$1.0 \cdot 10^{-02}$	$2.4103 \cdot 10^{+00}$	$1.8049 \cdot 10^{+00}$	$1.0163 \cdot 10^{+00}$
$5.0 \cdot 10^{-02}$	$1.4223 \cdot 10^{+00}$	$1.4575 \cdot 10^{+00}$	$8.5959 \cdot 10^{-01}$
$1.0 \cdot 10^{-01}$	$8.5836 \cdot 10^{-01}$	$1.0315 \cdot 10^{+00}$	$5.9413 \cdot 10^{-01}$
$2.0 \cdot 10^{-01}$	$3.4550 \cdot 10^{-01}$	$5.8112 \cdot 10^{-01}$	$2.9304 \cdot 10^{-01}$
$3.0 \cdot 10^{-01}$	$1.2159 \cdot 10^{-01}$	$3.5500 \cdot 10^{-01}$	$1.3022 \cdot 10^{-01}$
$4.0 \cdot 10^{-01}$	$3.5427 \cdot 10^{-02}$	$2.2467 \cdot 10^{-01}$	$4.9424 \cdot 10^{-02}$
$5.0 \cdot 10^{-01}$	$8.7151 \cdot 10^{-03}$	$1.4012 \cdot 10^{-01}$	$1.5228 \cdot 10^{-02}$
$6.0 \cdot 10^{-01}$	$2.0155 \cdot 10^{-03}$	$8.1569 \cdot 10^{-02}$	$3.4896 \cdot 10^{-03}$
$7.0 \cdot 10^{-01}$	$4.9631 \cdot 10^{-04}$	$4.1424 \cdot 10^{-02}$	$5.0279 \cdot 10^{-04}$
$8.0 \cdot 10^{-01}$	$1.0723 \cdot 10^{-04}$	$1.6180 \cdot 10^{-02}$	$3.1295 \cdot 10^{-05}$
$9.0 \cdot 10^{-01}$	$9.8900 \cdot 10^{-06}$	$3.3055 \cdot 10^{-03}$	$2.6762 \cdot 10^{-07}$

Table 36: Same as table 25: FFNS, $\mu_F^2 = 10^4 \text{ GeV}^2$, $\mu_R^2/\mu_F^2 = 2$, $\alpha_s(\mu_F^2) = 0.0982996$.

This script will automatically produce the relevant numbers and plots. Note that a previous installation of the **APFEL** library version 2.3.0 or higher and the **Gnuplot** plotting tool is required. For the installation of **APFEL** please refer to:

<http://apfel.hepforge.org/download.html>

References

- [1] J. C. Collins and D. E. Soper, *Back-To-Back Jets in QCD*, *Nucl.Phys.* **B193** (1981) 381. Erratum-ibid. B213 (1983) 545.
- [2] J. C. Collins and D. E. Soper, *Parton Distribution and Decay Functions*, *Nucl.Phys.* **B194** (1982) 445.
- [3] S. Albino, F. Anulli, F. Arleo, D. Z. Besson, W. K. Brooks, et al., *Parton fragmentation in the vacuum and in the medium*, [arXiv:0804.2021](#).
- [4] S. Albino, *The Hadronization of partons*, *Rev.Mod.Phys.* **82** (2010) 2489–2556, [[arXiv:0810.4255](#)].
- [5] J. C. Collins, D. E. Soper, and G. F. Sterman, *Factorization of Hard Processes in QCD*, *Adv.Ser.Direct.High Energy Phys.* **5** (1988) 1–91, [[hep-ph/0409313](#)].
- [6] V. Gribov and L. Lipatov, *Deep inelastic ep scattering in perturbation theory*, *Sov.J.Nucl.Phys.* **15** (1972) 438–450.
- [7] L. Lipatov, *The parton model and perturbation theory*, *Sov.J.Nucl.Phys.* **20** (1975) 94–102.
- [8] G. Altarelli and G. Parisi, *Asymptotic Freedom in Parton Language*, *Nucl.Phys.* **B126** (1977) 298.
- [9] Y. L. Dokshitzer, *Calculation of the Structure Functions for Deep Inelastic Scattering and e^+e^- Annihilation by Perturbation Theory in Quantum Chromodynamics.*, *Sov.Phys.JETP* **46** (1977) 641–653.
- [10] **HERMES** Collaboration, A. Airapetian et al., *Multiplicities of charged pions and kaons from semi-inclusive deep-inelastic scattering by the proton and the deuteron*, *Phys.Rev.* **D87** (2013) 074029, [[arXiv:1212.5407](#)].
- [11] **COMPASS** Collaboration, N. Du Fresne Von Hohenesche, *Hadron multiplicities at COMPASS*, *PoS DIS2014* (2014) 209.
- [12] **Belle** Collaboration, M. Leitgab et al., *Precision Measurement of Charged Pion and Kaon Differential Cross Sections in e^+e^- Annihilation at $\sqrt{s} = 10.52\text{ GeV}$* , *Phys.Rev.Lett.* **111** (2013) 062002, [[arXiv:1301.6183](#)].
- [13] **BaBar** Collaboration, J. Lees et al., *Production of charged pions, kaons, and protons in e^+e^- annihilations into hadrons at $\sqrt{s} = 10.54\text{ GeV}$* , *Phys.Rev.* **D88** (2013) 032011, [[arXiv:1306.2895](#)].
- [14] **STAR** Collaboration, G. Agakishiev et al., *Identified hadron compositions in $p+p$ and $Au+Au$ collisions at high transverse momenta at $\sqrt{s_{NN}} = 200\text{ GeV}$* , *Phys.Rev.Lett.* **108** (2012) 072302, [[arXiv:1110.0579](#)].
- [15] **PHENIX** Collaboration, A. Adare et al., *Inclusive cross-section and double helicity asymmetry for π^0 production in pp collisions at $\sqrt{s} = 200\text{ GeV}$: Implications for the polarized gluon distribution in the proton*, *Phys.Rev.* **D76** (2007) 051106, [[arXiv:0704.3599](#)].

- [16] **CMS** Collaboration, S. Chatrchyan et al., *Charged particle transverse momentum spectra in pp collisions at $\sqrt{s} = 0.9$ and 7 TeV*, *JHEP* **1108** (2011) 086, [[arXiv:1104.3547](#)].
- [17] **CMS** Collaboration, S. Chatrchyan et al., *Study of high- p_T charged particle suppression in PbPb compared to pp collisions at $\sqrt{s_{NN}} = 2.76$ TeV*, *Eur.Phys.J.* **C72** (2012) 1945, [[arXiv:1202.2554](#)].
- [18] **ALICE** Collaboration, B. B. Abelev et al., *Energy Dependence of the Transverse Momentum Distributions of Charged Particles in pp Collisions Measured by ALICE*, *Eur.Phys.J.* **C73** (2013), no. 12 2662, [[arXiv:1307.1093](#)].
- [19] W. Giele, E. N. Glover, I. Hinchliffe, J. Huston, E. Laenen, et al., *The QCD / SM working group: Summary report*, [hep-ph/0204316](#).
- [20] M. Dittmar, S. Forte, A. Glazov, S. Moch, S. Alekhin, et al., *Working Group I: Parton distributions: Summary report for the HERA LHC Workshop Proceedings*, [hep-ph/0511119](#).
- [21] V. Bertone, S. Carrazza, and J. Rojo, *APFEL: A PDF Evolution Library with QED corrections*, *Comput.Phys.Commun.* **185** (2014) 1647–1668, [[arXiv:1310.1394](#)].
- [22] S. Carrazza, A. Ferrara, D. Palazzo, and J. Rojo, *APFEL Web: a web-based application for the graphical visualization of parton distribution functions*, [arXiv:1410.5456](#).
- [23] M. Botje, *QCDNUM: Fast QCD Evolution and Convolution*, *Comput.Phys.Commun.* **182** (2011) 490–532, [[arXiv:1005.1481](#)].
- [24] M. Hirai and S. Kumano, *Numerical solution of Q^2 evolution equations for fragmentation functions*, *Comput.Phys.Commun.* **183** (2012) 1002–1013, [[arXiv:1106.1553](#)].
- [25] M. Hirai, S. Kumano, T.-H. Nagai, and K. Sudoh, *Determination of fragmentation functions and their uncertainties*, *Phys.Rev.* **D75** (2007) 094009, [[hep-ph/0702250](#)].
- [26] S. Albino, B. Kniehl, and G. Kramer, *AKK Update: Improvements from New Theoretical Input and Experimental Data*, *Nucl.Phys.* **B803** (2008) 42–104, [[arXiv:0803.2768](#)].
- [27] D. de Florian, R. Sassot, M. Epele, R. J. Hernandez-Pinto, and M. Stratmann, *Parton-to-Pion Fragmentation Reloaded*, [arXiv:1410.6027](#).
- [28] W. Furmanski and R. Petronzio, *Singlet Parton Densities Beyond Leading Order*, *Phys.Lett.* **B97** (1980) 437.
- [29] R. K. Ellis, W. J. Stirling, and B. Webber, *QCD and collider physics*, *Camb.Monogr.Part.Phys.Nucl.Phys.Cosmol.* **8** (1996) 1–435.
- [30] M. Gluck, E. Reya, and A. Vogt, *Parton fragmentation into photons beyond the leading order*, *Phys.Rev.* **D48** (1993) 116. Erratum-ibid. D51 (1995) 1427.
- [31] A. Mitov and S.-O. Moch, *QCD Corrections to Semi-Inclusive Hadron Production in Electron-Positron Annihilation at Two Loops*, *Nucl.Phys.* **B751** (2006) 18–52, [[hep-ph/0604160](#)].
- [32] M. Stratmann and W. Vogelsang, *Next-to-leading order evolution of polarized and unpolarized fragmentation functions*, *Nucl.Phys.* **B496** (1997) 41–65, [[hep-ph/9612250](#)].
- [33] J. Binnewies, B. A. Kniehl, and G. Kramer, *Coherent description of $D^{*\pm}$ production in e^+e^- and low Q^2 ep collisions*, *Z.Phys.* **C76** (1997) 677–688, [[hep-ph/9702408](#)].
- [34] A. Mitov, *A New method for calculating differential distributions directly in Mellin space*, *Phys.Lett.* **B643** (2006) 366–373, [[hep-ph/0511340](#)].

- [35] A. Mitov, S. Moch, and A. Vogt, *Next-to-Next-to-Leading Order Evolution of Non-Singlet Fragmentation Functions*, *Phys.Lett.* **B638** (2006) 61–67, [[hep-ph/0604053](#)].
- [36] S. Moch and A. Vogt, *On third-order timelike splitting functions and top-mediated Higgs decay into hadrons*, *Phys.Lett.* **B659** (2008) 290–296, [[arXiv:0709.3899](#)].
- [37] A. Almasy, S. Moch, and A. Vogt, *On the Next-to-Next-to-Leading Order Evolution of Flavour-Singlet Fragmentation Functions*, *Nucl.Phys.* **B854** (2012) 133–152, [[arXiv:1107.2263](#)].
- [38] J. Blumlein, V. Ravindran, and W. van Neerven, *On the Drell-Levy-Yan relation to $\mathcal{O}(\alpha_s^2)$* , *Nucl.Phys.* **B586** (2000) 349–381, [[hep-ph/0004172](#)].
- [39] P. Rijken and W. van Neerven, *$\mathcal{O}(\alpha_s^2)$ contributions to the longitudinal fragmentation function in e^+e^- annihilation*, *Phys.Lett.* **B386** (1996) 422–428, [[hep-ph/9604436](#)].
- [40] P. Rijken and W. van Neerven, *$\mathcal{O}(\alpha_s^2)$ contributions to the asymmetric fragmentation function in e^+e^- annihilation*, *Phys.Lett.* **B392** (1997) 207–215, [[hep-ph/9609379](#)].
- [41] P. Rijken and W. van Neerven, *Higher order QCD corrections to the transverse and longitudinal fragmentation functions in electron - positron annihilation*, *Nucl.Phys.* **B487** (1997) 233–282, [[hep-ph/9609377](#)].
- [42] E. Remiddi and J. Vermaseren, *Harmonic polylogarithms*, *Int.J.Mod.Phys.* **A15** (2000) 725–754, [[hep-ph/9905237](#)].
- [43] J. Blumlein, *Algebraic relations between harmonic sums and associated quantities*, *Comput.Phys.Commun.* **159** (2004) 19–54, [[hep-ph/0311046](#)].
- [44] S. Albino, *Analytic Continuation of Harmonic Sums*, *Phys.Lett.* **B674** (2009) 41–48, [[arXiv:0902.2148](#)].
- [45] See <http://www.liv.ac.uk/~avogt/split.html>.
- [46] J. Blumlein and V. Ravindran, *$\mathcal{O}(\alpha_s^2)$ Timelike Wilson Coefficients for Parton-Fragmentation Functions in Mellin Space*, *Nucl.Phys.* **B749** (2006) 1–24, [[hep-ph/0604019](#)].
- [47] A. Vogt, *Efficient evolution of unpolarized and polarized parton distributions with QCD-PEGASUS*, *Comput.Phys.Commun.* **170** (2005) 65–92, [[hep-ph/0408244](#)].
- [48] J. Abate and P. Valko, *Multi-precision Laplace transform inversion*, *International Journal for Numerical Methods in Engineering* **60** (2004) 979993.
- [49] R. D. Ball, L. Del Debbio, S. Forte, A. Guffanti, J. I. Latorre, et al., *A first unbiased global NLO determination of parton distributions and their uncertainties*, *Nucl.Phys.* **B838** (2010) 136–206, [[arXiv:1002.4407](#)].
- [50] M. Cacciari, P. Nason, and C. Oleari, *Crossing heavy-flavor thresholds in fragmentation functions*, *JHEP* **0510** (2005) 034, [[hep-ph/0504192](#)].
- [51] **The NNPDF Collaboration**, R. D. Ball et al., *Parton distributions for the LHC Run II*, [[arXiv:1410.8849](#)].
- [52] **The NNPDF Collaboration**, E. R. Nocera, R. D. Ball, S. Forte, G. Ridolfi, and J. Rojo, *A first unbiased global determination of polarized PDFs and their uncertainties*, *Nucl.Phys.* **B887** (2014) 276–308, [[arXiv:1406.5539](#)].